Report No. K-TRAN: KU-10-8 ▪ FINAL REPORT ▪ February 2013

Assessing LiDAR Elevation Data for KDOT Applications

C. Bryan Young, Ph.D., P.E.
The University of Kansas

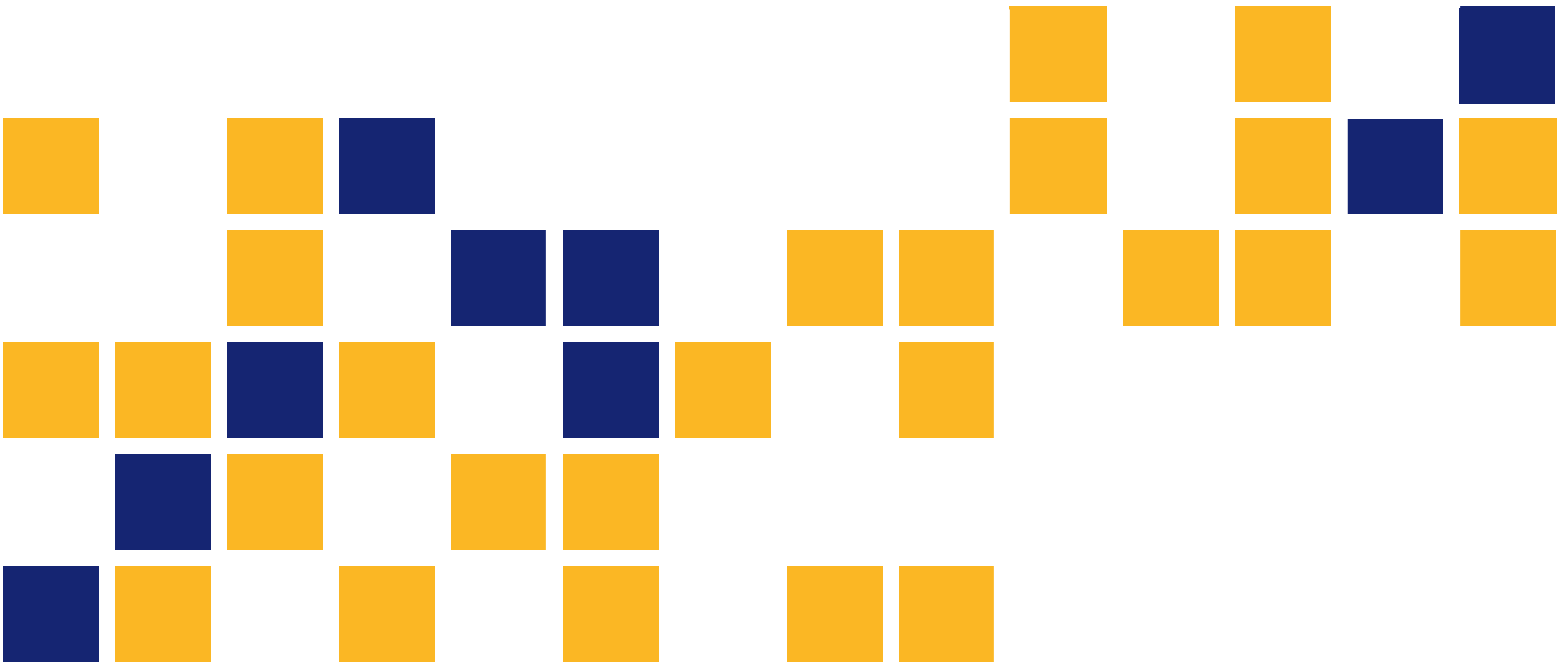

A cooperative transportation research program between
Kansas Department of Transportation,
Kansas State University Transportation Center, and
The University of Kansas

Kansas Department of Transportation

This page intentionally left blank.

1 Report No. K-TRAN: KU-10-8	**2 Government Accession No.**	**3 Recipient Catalog No.**
4 Title and Subtitle Assessing LiDAR Elevation Data for KDOT Applications		**5 Report Date** February 2013
		6 Performing Organization Code
7 Author(s) C. Bryan Young, Ph.D., P.E.		**8 Performing Organization Report No.**
9 Performing Organization Name and Address University of Kansas Civil, Environmental & Architectural Engineering Department 1530 West 15th Street Lawrence, Kansas 66045-7609		**10 Work Unit No. (TRAIS)**
		11 Contract or Grant No. C1836
12 Sponsoring Agency Name and Address Kansas Department of Transportation Bureau of Materials and Research 700 SW Harrison Street Topeka, Kansas 66603-3745		**13 Type of Report and Period Covered** Final Report September 2009–June 2012
		14 Sponsoring Agency Code RE-0537-01

15 Supplementary Notes

LiDAR-based elevation surveys are a cost-effective means for mapping topography over large areas. LiDAR surveys use an airplane-mounted or ground-based laser radar unit to scan terrain. Post-processing techniques are applied to remove vegetation and reveal the bare-earth elevations. In recent years, LiDAR hardware and processing technologies have improved greatly. LiDAR surveys are now cost-competitive with traditional aerial topographic surveys and offer the capability to produce very high resolutions (potentially over 50 points per m^2 with <10 cm vertical accuracy for airborne systems).

LiDAR survey data may not replace traditional ground-based survey for applications that require centimeter or sub-centimeter accuracy, but the data available from these surveys may be perfect for many engineering applications. One such application is hydraulic modeling with HEC-RAS. Hydraulic models, used for flood-plain mapping and the evaluation of bridge backwater effects, require detailed elevation maps for the stream channel and floodplain. These data are difficult to obtain using traditional aerial survey techniques due to riparian vegetation that obstructs the view of the stream channel. Another potential application for LiDAR data is earthwork calculations (cut/fill analysis) for preliminary route planning purposes. Because LiDAR surveys are fairly new, the applications and limitations of these data have not been explored. This report summarizes an extensive literature review of LiDAR applications. In addition, this report documents the University of Kansas's experience with a Riegl terrestrial LiDAR system.

17 Key Words LiDAR, Mapping, Survey		**18 Distribution Statement** No restrictions. This document is available to the public through the National Technical Information Service www.ntis.gov.	
19 Security Classification (of this report) Unclassified	**20 Security Classification (of this page)** Unclassified	**21 No. of pages** 74	**22 Price**

Form DOT F 1700.7 (8-72)

Assessing LiDAR Elevation Data for KDOT Applications

Final Report

Prepared by

C. Bryan Young, Ph.D., P.E.
The University of Kansas

A Report on Research Sponsored by

THE KANSAS DEPARTMENT OF TRANSPORTATION
TOPEKA, KANSAS
and
THE UNIVERSITY OF KANSAS
LAWRENCE, KANSAS

February 2013

PREFACE

The Kansas Department of Transportation's (KDOT) Kansas Transportation Research and New-Developments (K-TRAN) Research Program funded this research project. It is an ongoing, cooperative and comprehensive research program addressing transportation needs of the state of Kansas utilizing academic and research resources from KDOT, Kansas State University and the University of Kansas. Transportation professionals in KDOT and the universities jointly develop the projects included in the research program.

NOTICE

The authors and the state of Kansas do not endorse products or manufacturers. Trade and manufacturers names appear herein solely because they are considered essential to the object of this report.

This information is available in alternative accessible formats. To obtain an alternative format, contact the Office of Transportation Information, Kansas Department of Transportation, 700 SW Harrison, Topeka, Kansas 66603-3754 or phone (785) 296-3585 (Voice) (TDD).

DISCLAIMER

The contents of this report reflect the views of the authors who are responsible for the facts and accuracy of the data presented herein. The contents do not necessarily reflect the views or the policies of the state of Kansas. This report does not constitute a standard, specification or regulation.

Acknowledgements

This project was supported by the Kansas Department of Transportation (KDOT) through the Kansas Transportation Research and New Developments (K-TRAN) Program. Mike Orth, P.E., and Jim Richardson, P.E., of KDOT served as project monitors. The author sincerely appreciates the support of KDOT and the contributions of Mr. Orth and Mr. Richardson.

Abstract

LiDAR-based elevation surveys are a cost-effective means for mapping topography over large areas. LiDAR surveys use an airplane-mounted or ground-based laser radar unit to scan terrain. Post-processing techniques are applied to remove vegetation and reveal the bare-earth elevations. In recent years, LiDAR hardware and processing technologies have improved greatly. LiDAR surveys are now cost-competitive with traditional aerial topographic surveys and offer the capability to produce very high resolutions (potentially over 50 points per m^2 with <10 cm vertical accuracy for airborne systems).

LiDAR survey data may not replace traditional ground-based survey for applications that require centimeter or sub-centimeter accuracy, but the data available from these surveys may be perfect for many engineering applications. One such application is hydraulic modeling with HEC-RAS. Hydraulic models, used for flood-plain mapping and the evaluation of bridge backwater effects, require detailed elevation maps for the stream channel and floodplain. These data are difficult to obtain using traditional aerial survey techniques due to riparian vegetation that obstructs the view of the stream channel. Another potential application for LiDAR data is earthwork calculations (cut/fill analysis) for preliminary route planning purposes. Because LiDAR surveys are fairly new, the applications and limitations of these data have not been explored. This report summarizes an extensive literature review of LiDAR applications. In addition, this report documents the University of Kansas's experience with a Riegl terrestrial LiDAR system.

Table of Contents

List of Tables

List of Figures

Chapter 1: Introduction

1.1 Background and Justification

Application of Light Detection And Ranging (LiDAR) technology to transportation-related projects has increased drammatically over the past ten years. LiDAR-based elevation surveys are a cost-effective means for mapping topography over large areas. LiDAR surveys use an airborne or ground-based laser to scan terrain. Post-processing techniques are applied to remove vegetation and reveal the bare-earth elevations. In recent years, LiDAR hardware and processing technologies have improved greatly. LiDAR surveys are now cost-competitive with traditional survey techniques (total station and photogrammetric) and offer the capability to produce very high resolutions (potentially over 50 points per m^2 with <10 cm vertical accuracy for airborne systems).

Airborne LiDAR survey data may not replace traditional ground-based survey for applications that require sub-decimeter accuracy, but the data available from these surveys may be perfect for many engineering applications. One such application is hydraulic modeling with HEC-RAS. Hydraulic models, used for floodplain mapping and the evaluation of bridge backwater effects, require detailed elevation maps for the stream channel and floodplain. These data are difficult to obtain using traditional aerial survey techniques due to riparian vegetation that obstructs the view of the stream channel. Another potential application for LIDAR data is earthwork calculations (cut/fill analysis) for preliminary route planning purposes. Because LIDAR surveys are fairly new, the applications and limitations of these data have not been explored. This report summarizes the state-of-the-art of LiDAR data collection and applications.

1.2 Overview of LiDAR Technology

There are three major classes of LiDAR scanners: DIfferential Absorption LiDAR (DIAL), Doppler, and range detection. DIAL systems, also referred to as probing LiDAR, are used to measure the atmospheric concentration of a specific gas (Baltsavias 1999). DIAL systems make use of two laser wavelengths selected such that the chemical of interest absorbs one wavelength but not the other. The difference in the return of the two wavelengths can be compared to infer the concentration of the gas (Tao and Hu 2002). DIAL systems have been used

to estimate evapotranspiration from the land surface and to monitor air pollution due to traffic emissions.

Doppler LiDAR is commonly used for velocity measurement. The most common application of Doppler LiDAR is in speed guns (Tao and Hu 2002).

Range-detection LiDAR units use either a time-of-travel or phase-shift approach to estimating distance traveled from the LiDAR unit to the target. Time-of-travel laser scanners are used for long-range applications. Phase-shift laser scanners measure the phase shift in the return signal to detect distance. Phase-shift LiDAR systems are typically faster, more accurate, but limited in range (Liu et al. 2011). This report concentrates on the applications of range-detection LiDAR for transportation projects.

1.3 Range-Detection LiDAR Acquisition Systems

Range-detection LiDAR systems can be deployed three different ways: Airborne Laser Scanning (ALS), Mobile Laser Scanning (MLS), and Terrestrial Laser Scanning (TLS).

1.3.1 Airborne Laser Scanning (ALS)

ALS is also referred to as Airborne Laser Terrain Mapping (ALTM) in the literature. ALS will be used throughout this report. ALS uses a time-of-travel laser scanner mounted on a fixed-wing plane or helicopter. The x, y, and z coordinates of the target are computed using the laser-determined range, the angle of the laser, and the location and orientation of the aircraft. The location and orientation (pitch, roll, yaw) of the aircraft are determined using a combination of Global Positioning System (GPS) coordinates and an Inertial Navigation System (INS), also referred to as Inertial Measurement Unit (IMU) (Veneziano et al. 2002).

ALS surveys for mapping topography are typically conducted from a flight elevation of 500 m to 1500 m above ground level (AGL). Most highway surveys are flown at 500 m (Uddin 2002) to increase point density. The narrower swath incurred by lower flight elevations is not problematic for mapping linear features such as highway corridors.

Typical ALS surveys can map over 20,000 acres in a single day (Uddin 2002). Actual coverage is a function of flight elevation and speed, swath overlap, and distance from the operating airport.

Airborne LiDAR systems typically emit 10,000 to 70,000 pulses of light per second (Hodgson and Bresnahan 2004). Despite the very short pulse duration, each pulse is approximately 200 cm in length. Emitted as a point of light from the LiDAR unit, the pulse diverges with distance. Although the angle of divergence is quite small, the pulse may cover anywhere from 24 to 60 cm by the time it hits the ground (Hodgson and Bresnahan 2004). As such, the LiDAR return is not actually giving the distance to a point on the ground. Instead, the LiDAR system will record multiple return ranges (from the top of vegetation to the ground). Figure 1.1 and 1.2 illustrate cross sections from ALS survey data which clearly show elevation and ground returns.

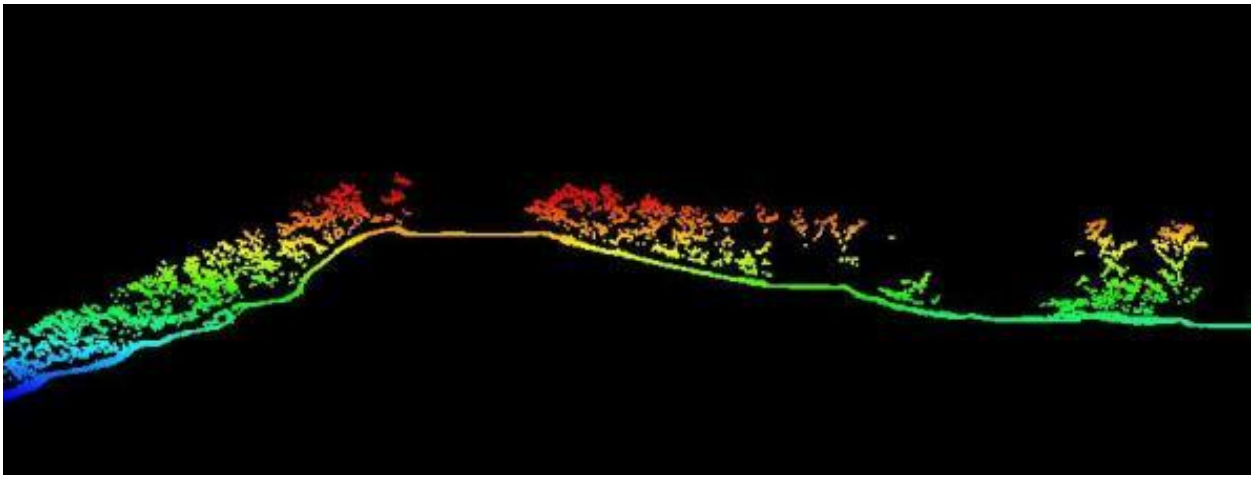

(Source: PhotoScience, Inc.)

FIGURE 1.1
Cross Section of an ALS Survey, Showing Vegetation and Ground Returns

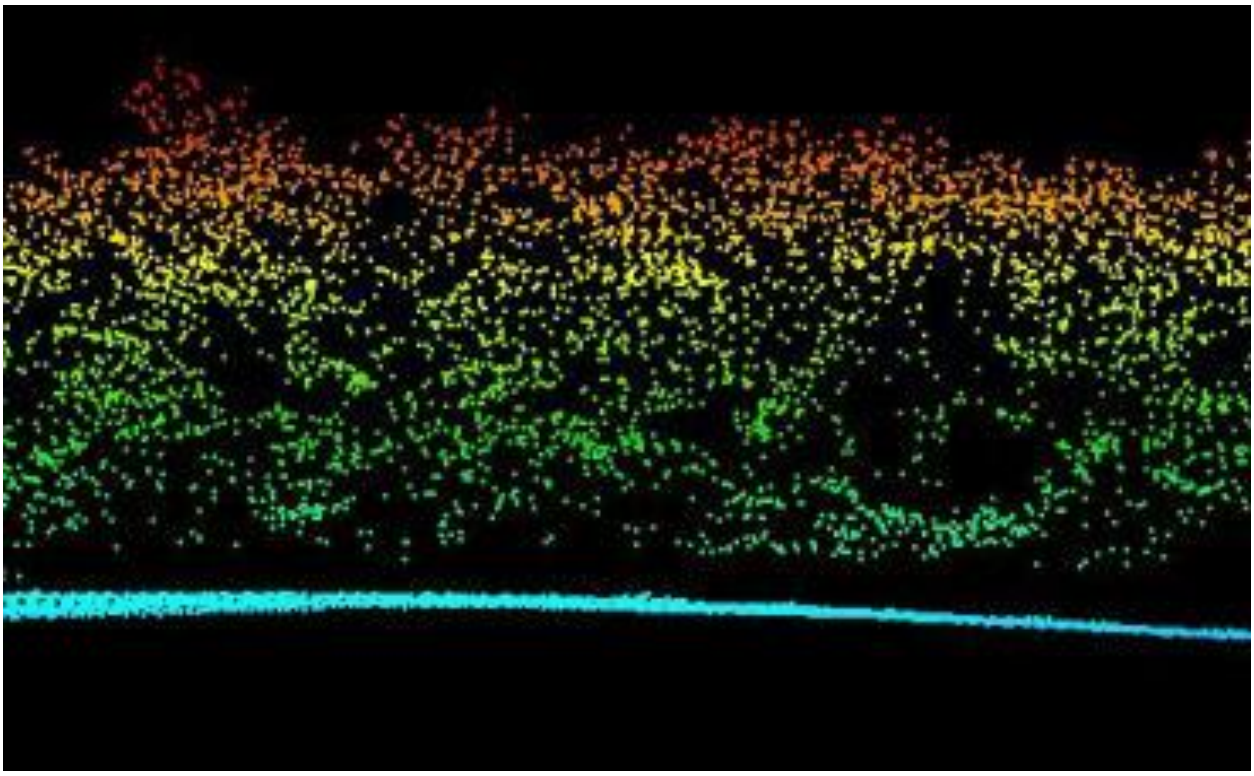

(Source: PhotoScience, Inc.)

FIGURE 1.2
Vegetation and Ground Returns

Differential LiDAR, or dual-frequency LiDAR, may be used on an airborne platform for bathymetric mapping (Baltsavias 1999). Dual-frequency LiDAR uses one wavelength that is readily reflected by water and one that penetrates water to map the bathymetry of shallow rivers, lakes, and coastal regions.

Modern laser scanners can collect up to 50 points/m^2 from aircraft (Zhou and Vosselman 2012).

1.3.2 Mobile Laser Scanning (MLS)

MLS is very similar in nature to ALS. The range-detection LiDAR unit is mounted on a ground-based vehicle (e.g. van, truck, or train). The LiDAR unit is coupled with a GPS and INS to track the location of the vehicle. Depending on the desired range of the LiDAR, either phase-shift or time-of-travel LiDAR can be used for mobile applications.

Lato et al. (2009) describe a typical MLS collection system. In this case, the LiDAR scanner was mounted in a pod above the bed of a high-rail pickup truck capable of traveling on road or rail. The scanner used had a maximum range of 200 m. The point density from the mobile LiDAR platform ranged from 50 to 500 points/m^2, depending on vehicle speed and laser scanner settings. As with ALS, a GPS and INS were used to reference the location of the vehicle. Vibrations on the order of mm to cm in the vehicle complicate precise determination of location. The GPS used by Lato et al. (2009) recorded one location per second, while the INS collected 2000 readings per second. However, the LiDAR made 40,000 readings per second. So, accurate interpolation between the GPS fixes using INS data is critical to accuracy. Careful configuration can allow positioning of the vehicle within 5 cm.

Modern laser scanners permit the collection of over 1000 points/m^2 using a vehicle-mounted platform (Zhou and Vosselman 2012).

1.3.3 Terrestrial Laser Scanning (TLS)

TLS employs either time-of-travel or phase-shift LiDAR on a stationary, ground-based platform. TLS is most commonly used for very small study areas where accuracy is critical. Examples of TLS applications include bridge and structure mapping (interior and exterior) as well as site-specific surveys. Most often, scans are generated from multiple scanner positions and results are tied together using dedicated reference points or tie points. Tie points are usually reflective prisms, cylinders, or discs that are positioned around the study area. Usually a minimum of four tie points is required to reference adjacent images.

1.4 Standards

The American Society for Photogrammetry and Remote Sensing (ASPRS) requires vertical accuracy expressed as the root mean square error (RMSE) of 4.6 cm for generation of 0.5 m contours (Al-Durgham et al. 2010). Table 1.1 presents ASPRS vertical accuracy requirements for contour intervals from 0.5 to 10 ft (Flood 2004). FEMA requires a LiDAR-based DEM vertical RMSE < 15 cm for use in flood plain modeling and mapping (FEMA 2012).

TABLE 1.1
Vertical Accuracy Requirements for Generating Contour Maps Published by ASPRS

Contour Interval (ft)	RMSE (ft)	RMSE (cm)
0.5	0.15	4.60
1	0.30	9.25
2	0.61	18.5
4	1.22	37.0
5	1.52	46.3
10	3.04	92.7

(Source: Flood 2004)

1.5 Overview of Report

Chapter 2 presents applications and error estimates for LiDAR surveys. Chapter 3 covers the University of Kansas's (KU's) experience with a Riegl terrestrial laser scanner acquired in 2008. Chapter 4 presents the status of available LiDAR data for the State of Kansas. Chapter 5 covers recommendations and conclusions from this research project.

Note on units: this report uses a mixture of SI and US units to report as directly as possible the findings of other researchers on LiDAR applications. SI is most common for scientific and engineering research publications and is thus most prevalent throughout this report.

Chapter 2: Sample Applications of LiDAR Data

2.1 Local Applications

This section summarizes several local applications of LiDAR data. Images and information are presented here for qualitative purposes only. This report should not be perceived as giving real or implied endorsement for any specific firm or vendor.

2.1.1 Power Line Surveys

The most common application of LiDAR surveys has been the mapping of power distribution infrastructure. Utility companies are under federal mandate to study vegetation encroachment on power lines and other transmission components. Figures 2.1 through 2.5 show sample images from a variety of surveying and engineering firms.

The advantage of LiDAR for power corridor surveys is that the technology is able to map the location of very small features (i.e., power lines).

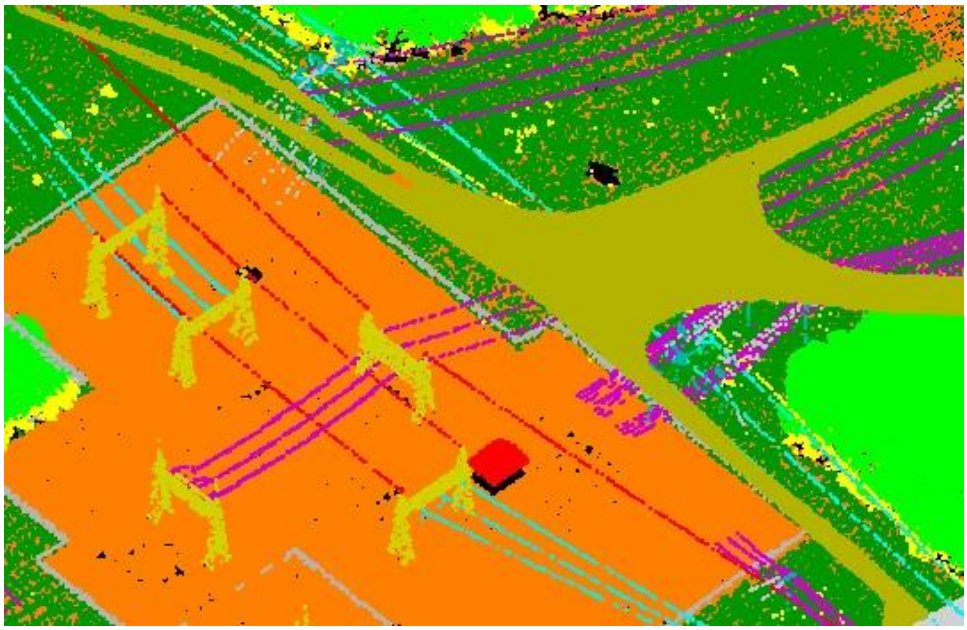

(Source: Black & Veatch)

FIGURE 2.1
LiDAR Mapping of Power Distribution Infrastructure

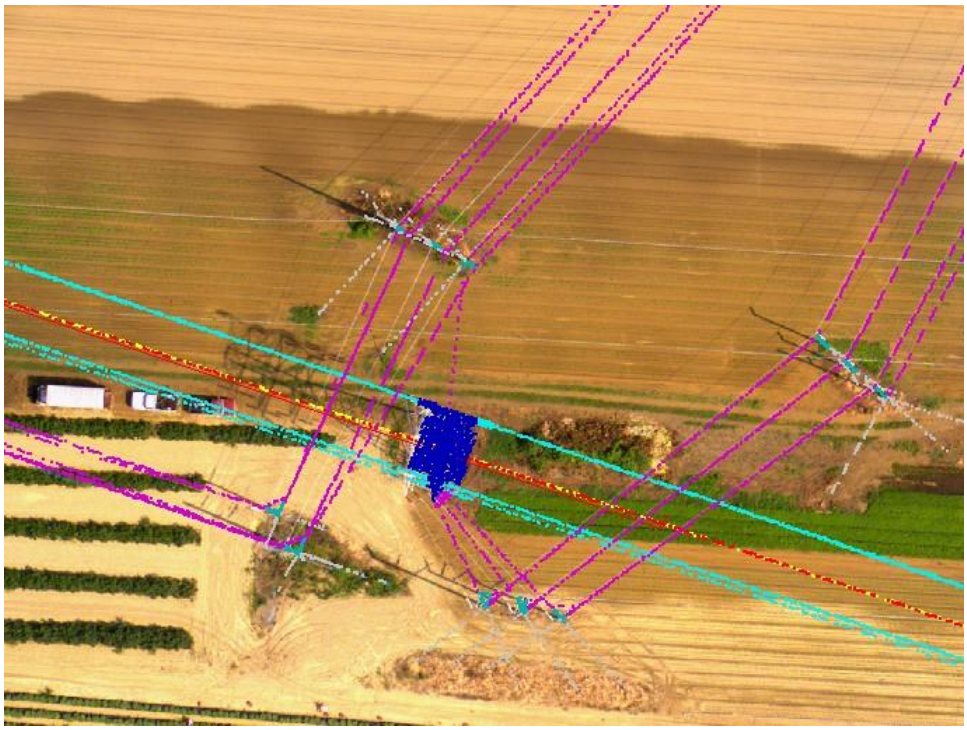

(Source: Black & Veatch)

FIGURE 2.2
LiDAR Mapping of Power Distribution Infrastructure

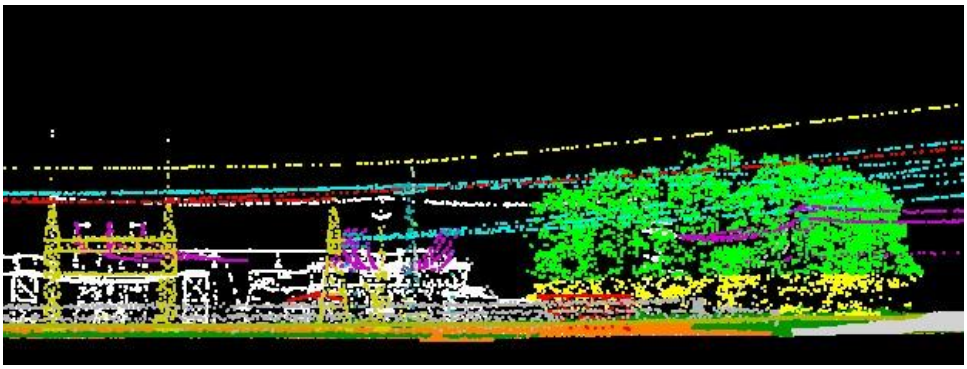

(Source: Black & Veatch)

FIGURE 2.3
LiDAR Mapping of Power Distribution Infrastructure

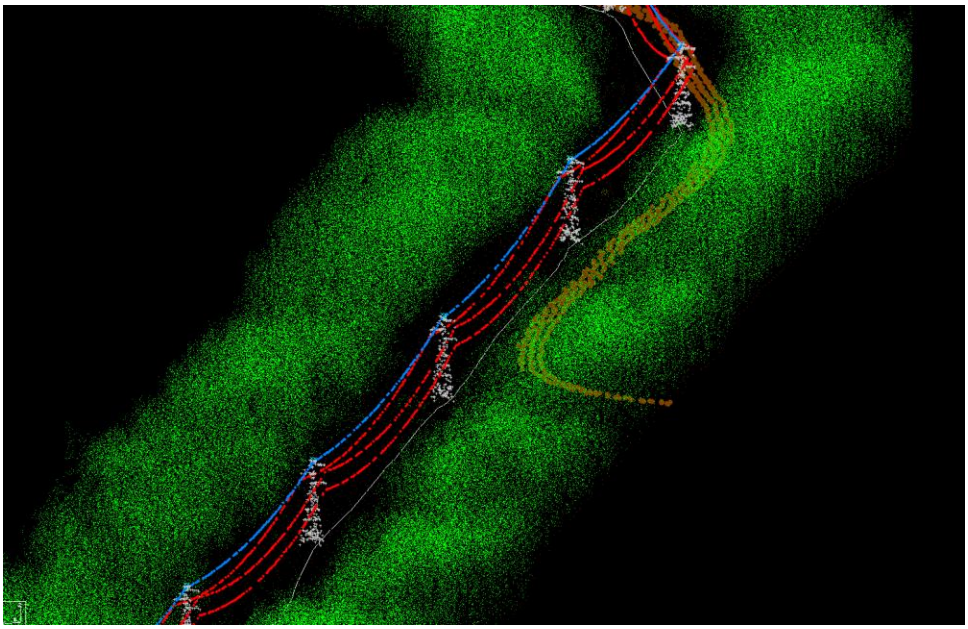

(Source: Burns & McDonnell)

FIGURE 2.4
LiDAR Mapping of Power Distribution Infrastructure

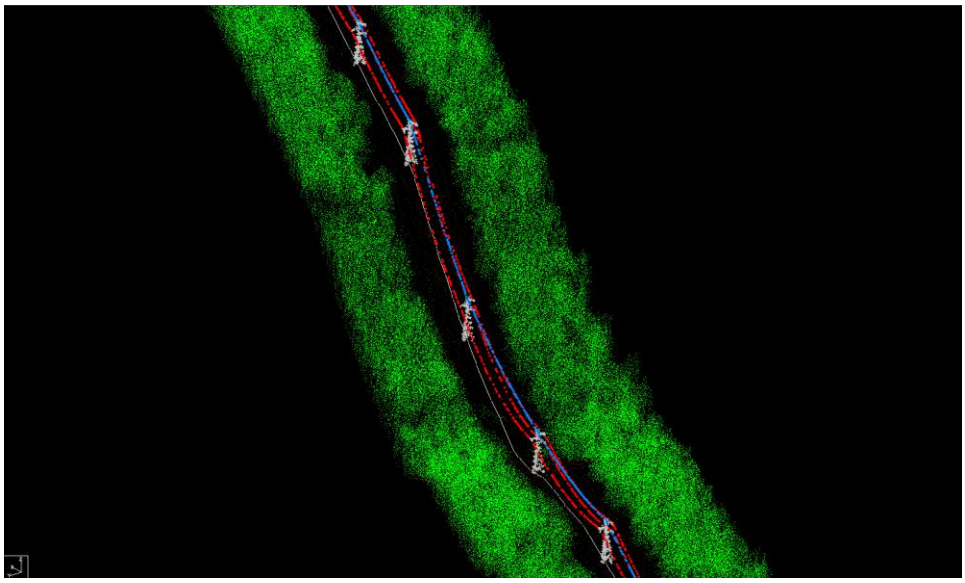

(Source: Burns & McDonnell)

FIGURE 2.6
LiDAR Mapping of Power Distribution Infrastructure

2.1.2 Urban Infrastructure Mapping

LiDAR is able to capture and map 3D structures, such as buildings, bridges, and other man-made infrastructure in urban environments. These maps can be useful for urban planning, flood plain mapping and risk analysis, as well as for studying cell phone or wireless internet distribution networks. Figures 2.6 and 2.7 illustrate the ability of LiDAR data collection and post processing to develop maps classifying object type. 3D point maps such as these can be used to construct 3D models of structures, as shown in Figure 2.8.

(Source: PhotoScience, Inc.)

FIGURE 2.6
LiDAR Mapping of Urban Area

,

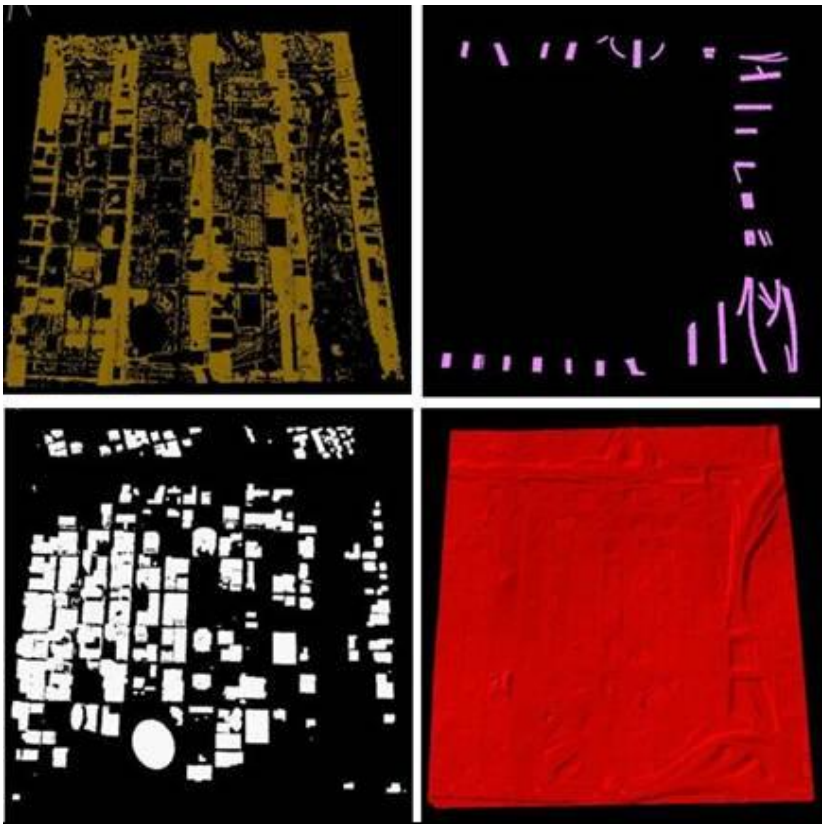

(Source: PhotoScience, Inc.)

FIGURE 2.7
LiDAR Mapping of Urban Area

(Source: PhotoScience, Inc.)

FIGURE 2.8
Development of 3D Structure Model with LiDAR Data

2.1.3 Floodplain Modeling and Mapping

ALS is frequently used in the development of hydrologic and hydraulic models for determining flood stage and mapping flood plains. Figure 2.9 shows a sample floodplain map with cross sections, contours, buildings, and background aerial photography. FEMA requires a vertical RMSE of < 15 cm for LiDAR for flood plain modeling.

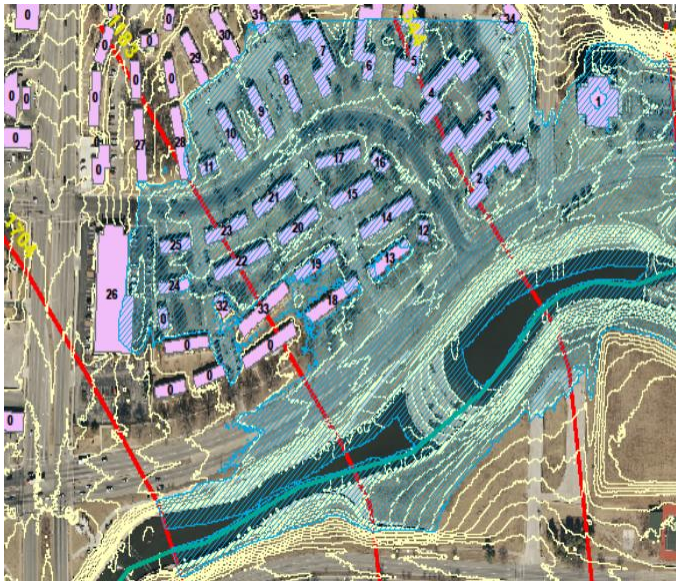

(Source: PhotoScience, Inc.)

FIGURE 2.9
LiDAR Used for Floodplain Modeling and Mapping

2.1.4 Building Models

TLS is commonly used to develop 3D models of building interiors for significant renovation projects of industrial facilities. Figures 2.10 and 2.11 show classified 3D point clouds mapping the interior of buildings. Advances in post-processing software allow the rapid conversion of 3D point clouds to 3D solid models.

Figures 2.12 through 2.14 show LiDAR imagery and the resulting solid model developed of the Kansas State Capitol for the ongoing renovation project. The 3D model was used to test for interferences between the temporary scaffolding structure and interior components of the dome.

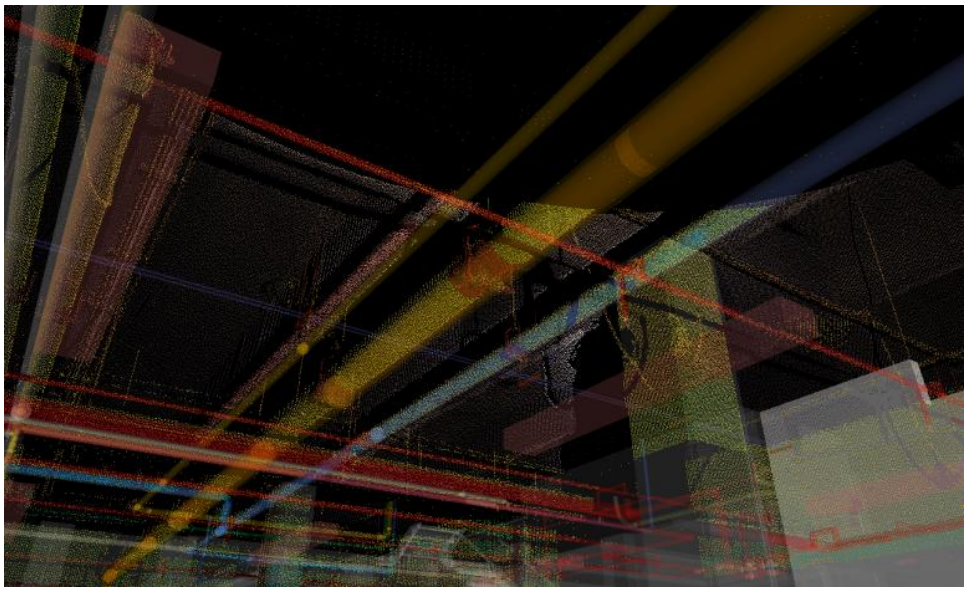

(Source: JE Dunn Construction)

FIGURE 2.10
LiDAR Mapping of Building Interior

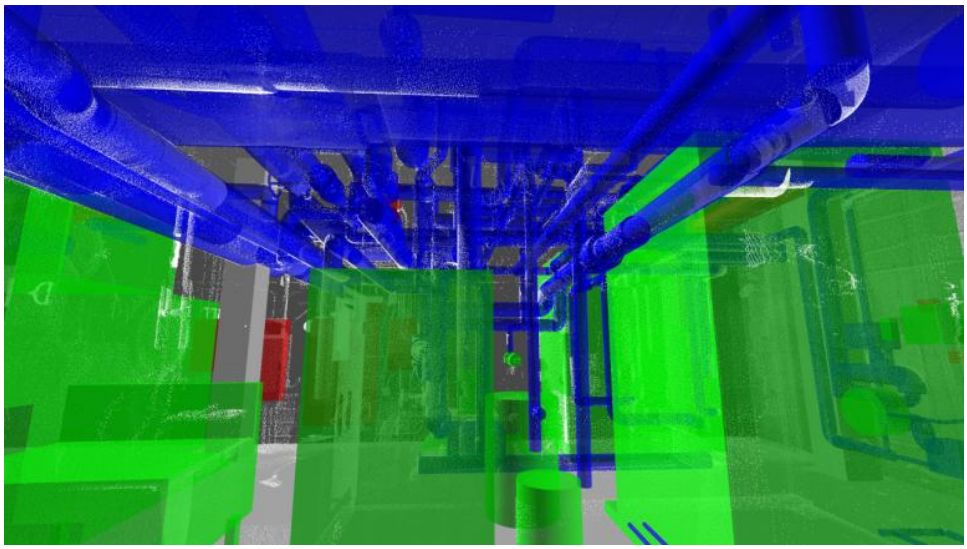

(Source: JE Dunn Construction)

FIGURE 2.11
LiDAR Mapping of Building Interior

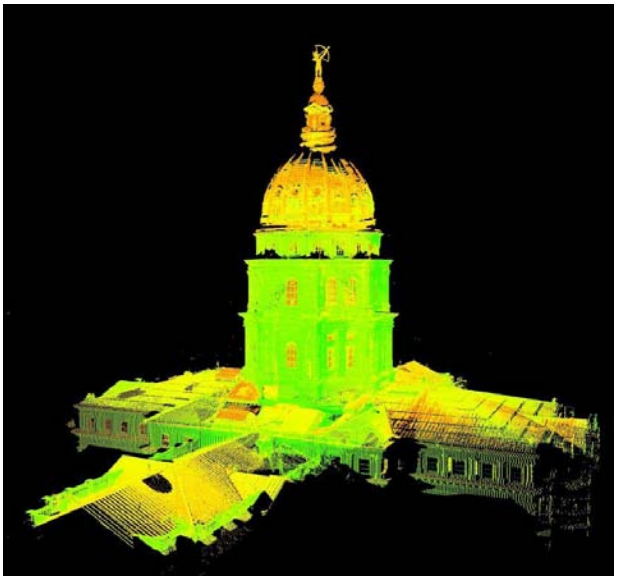

(Source: BHC Rhodes)

FIGURE 2.12
LiDAR Point Map of the Kansas State Capitol Building

(Source: BHC Rhodes)

FIGURE 2.13
LiDAR-Derived CAD Model of the Kansas State Capitol Building

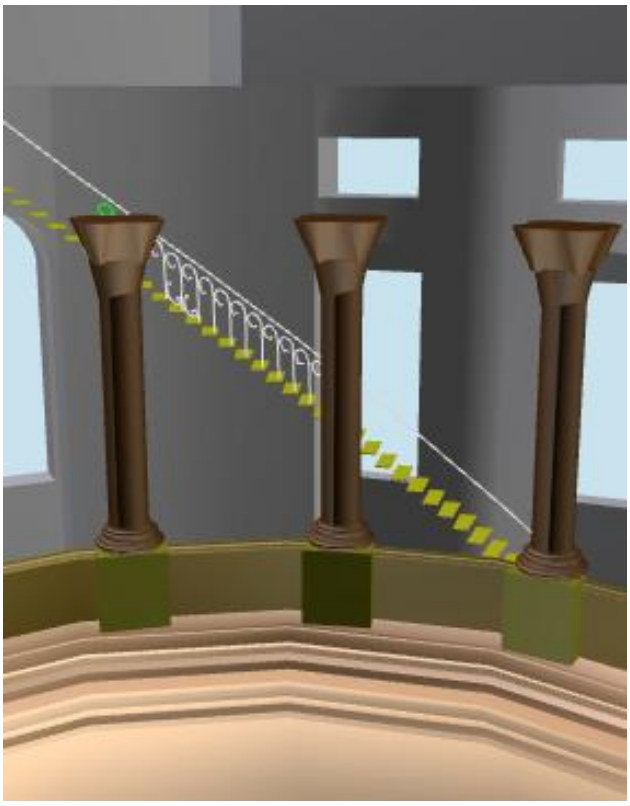

(Source: BHC Rhodes)

FIGURE 2.14
LiDAR-Derived CAD Model of the Kansas State Capitol Building, Interior View of the Dome

2.1.5 Construction Applications

TLS can be used to document as-built conditions, or to evaluate construction quality to ensure that construction specifications are met.

Figures 2.15 and 2.16 show a partial cross section of a 15 m tall monolithic concrete wall that was scanned using TLS to document and measure actual constructed dimensions. The wall was found to be out of plumb in multiple locations affecting a steel structure that was designed to attach to the wall at various points. LiDAR measurements were used to modify the steel framing and connections thus preventing tear-down and reconstruction of the structure. The LiDAR model was later used to measure and verify constructed dimensions of door and window openings. This task was not anticipated at the time of the LiDAR survey but was made possible by the volume of data collected.

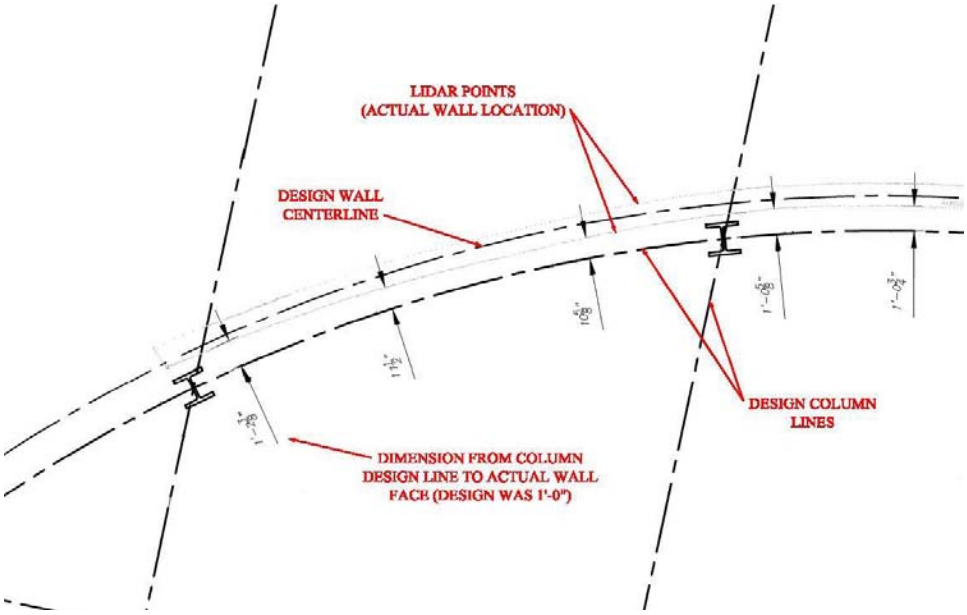

(Source: BHC Rhodes)

FIGURE 2.15
Comparison of LiDAR-Derived As-Built Measurements with Design Plans

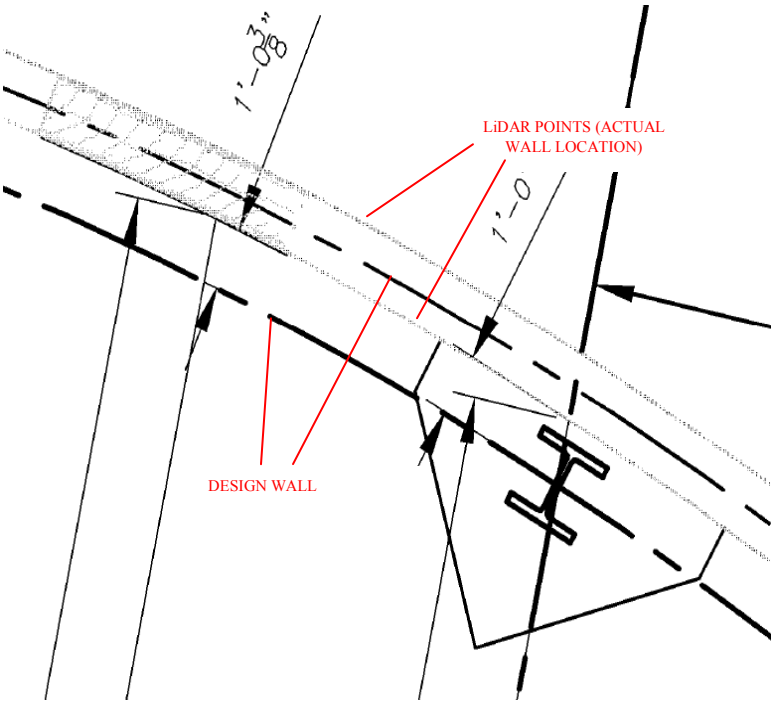

(Source: BHC Rhodes)

FIGURE 2.16
Comparison of LiDAR-Derived As-Built Measurements with Design Plans

Figure 2.17 shows a TLS point cloud generated for a subgrade certification. Point colors were used to show deviations of the surveyed points from the anticipated design surface. Blue indicates locations below the design grade, green indicates locations at the design grade, and red indicates locations above the design grade. The capability of LiDAR to perform a non-intrusive, detailed mapping of as-built conditions will need to be considered in the development of construction specifications.

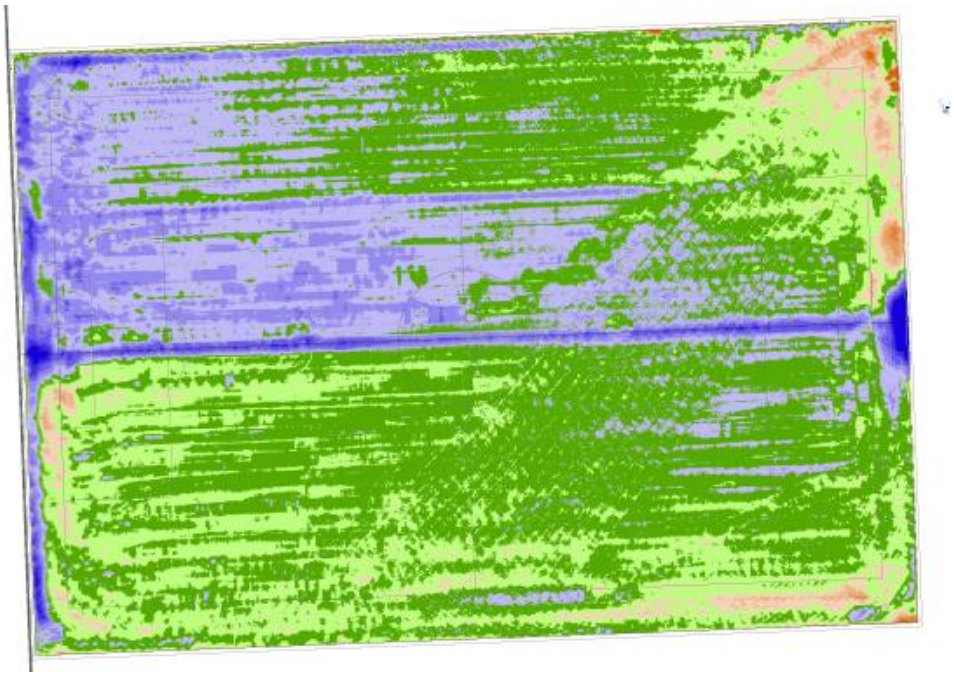

(Source: BHC Rhodes)

FIGURE 2.17
LiDAR Map for Subgrade Certification

Figures 2.18 through 2.20 show TLS data from a bridge structure. At the time of construction, there was significant concern whether the final girder sections would fit properly. LiDAR scans allowed a virtual test of fit. This application could have prevented an unnecessary highway closure.

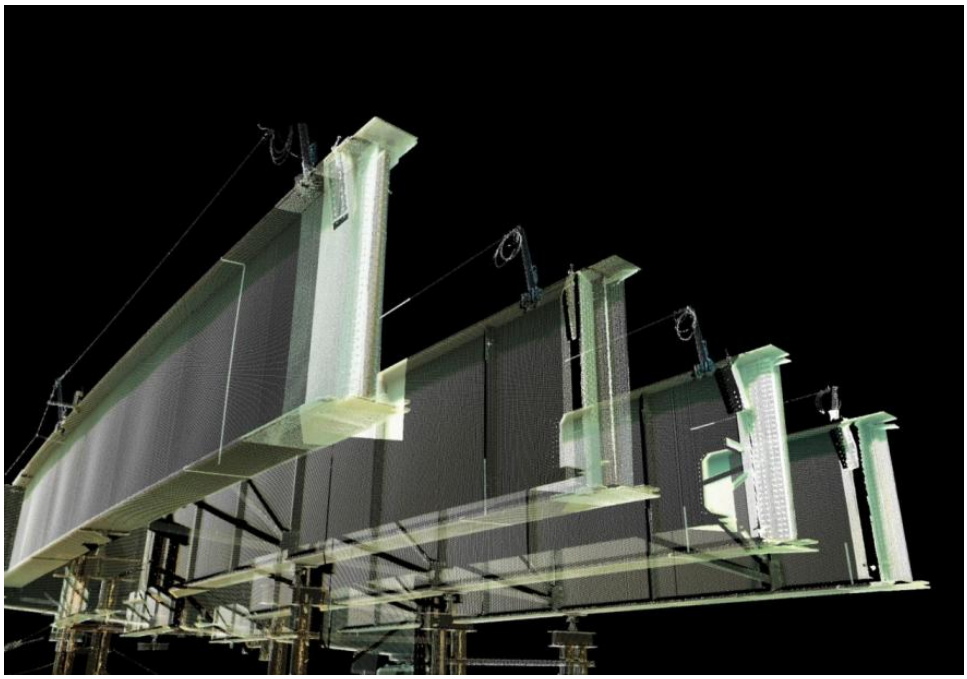

(Source: BHC Rhodes)

FIGURE 2.18
LiDAR-Generated Model of As-Built Bridge Structure

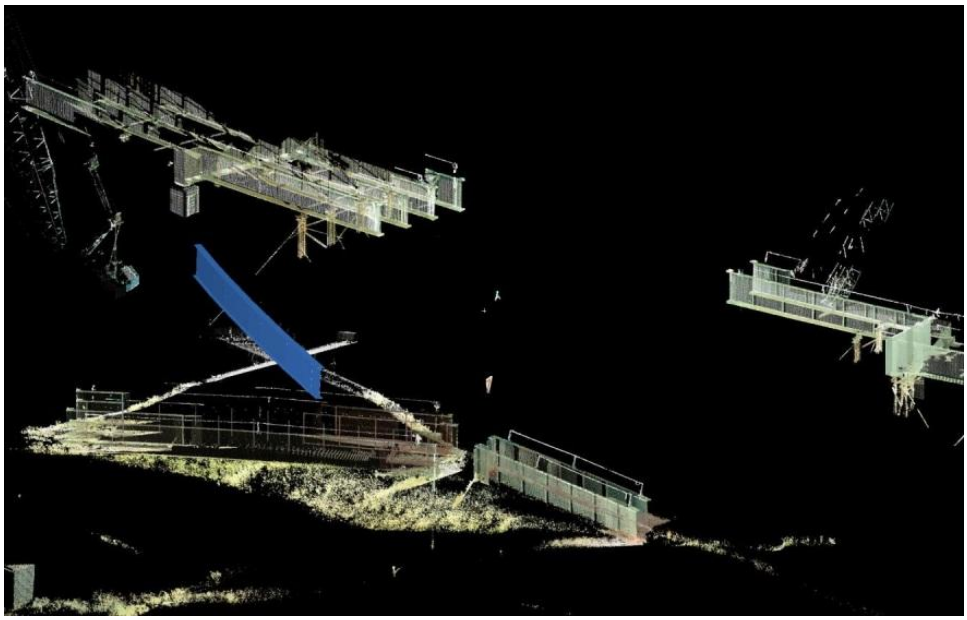

(Source: BHC Rhodes)

FIGURE 2.19
Virtual Test of Girder Fit, Girder Being Lifted into Place

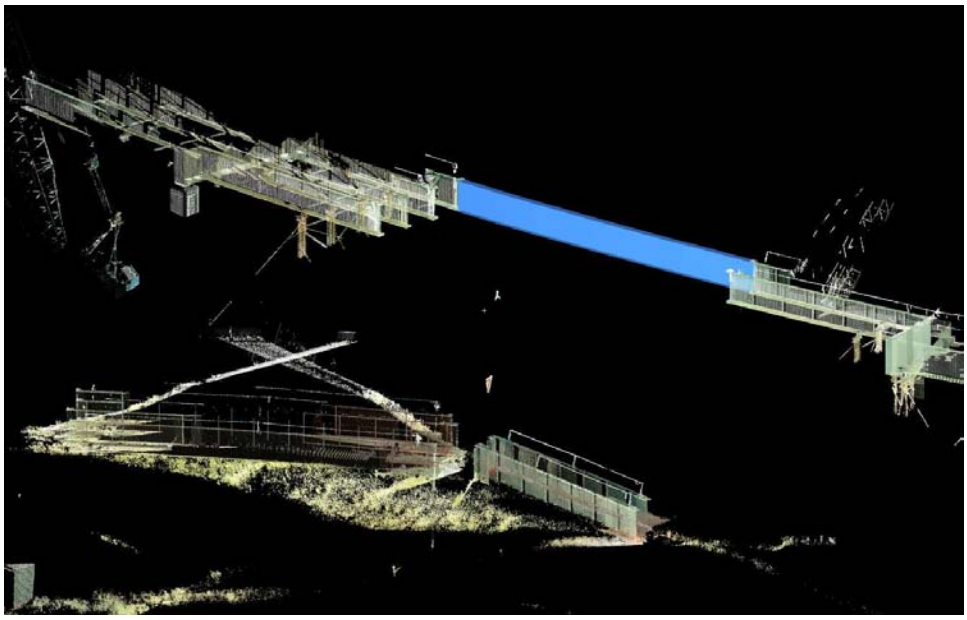

(Source: BHC Rhodes)

FIGURE 2.20
Virtual Test of Girder Fit, Girder in Place and Checked

2.2 Literature Review of Applications

Highway corridor mapping/cut-fill analysis: LiDAR has been used to map highway corridors for planning and design. ALS is ideal for the mapping of linear features (like highway corridors), but the real question remains whether ALS data are accurate enough for highway planning and design applications. Much of the literature on this topic is summarized in the section on LiDAR error analysis. Studies that focus on highway planning include (Uddin 2002), (Veneziano et al. 2004), (Paska and Ray 2007), and (O'Hara 2002)

Line of sight analysis: Khattak et al. (2003) studied driver sight lines at six intersections along the northern section of the IA-1 Solon Bypass in Iowa. ALS data were collected for this section of IA-1. Both first (usually top of vegetation) and last (ground) returns were used to construct a 3D representation of the ground, vegetation, buildings, and posts. The 3D LiDAR data were analyzed using line-of-sight analysis tools in ArcView GIS for visual obstructions as a driver approaches each intersection. The analysis identified a total of 66 potential obstructions. Field verification showed that 62 of these 66 were correctly identified by the LiDAR analysis. Three obstructions were noted during field verification that were not detected using the LiDAR survey. This line-of-sight analysis has not been automated to a high degree, and is time

consuming. However, LiDAR documentation of existing conditions may be useful for analyzing obstructions for accident locations.

In a related study, Khattak and Shamayleh (2005) used the IA-1 LiDAR data to identify sight-distance problems. The 3D LiDAR data were analyzed in a GIS environment to a) visually identify potential sight-distance problems and b) investigate potential problem spots with line-of-sight analysis in the GIS software. Khattak and Shamayleh (2005) concluded that LiDAR is useful for sight-distance studies, though the cost of data acquisition and processing may be barriers to wide-spread use. No direct comparisons were made with established sight-distance measurements; results of this study were purely qualitative.

Bridge clearance: LiDAR scanning has been used to map bridge clearance. Measurement of vertical clearance is challenging (Liu et al. 2011). Liu et al. (2009) developed a new algorithm to compute minimum clearance using terrestrial LiDAR observations. The algorithm, combined with a short-range LiDAR unit, has a stated accuracy on order of millimeters. Liu et al. (2011) used a Faro LS 880HE phase-based laser scanner with a range of 76 m (short range). The Faro scanner has a laser wavelength of 785 nm. Liu et al. (2011) evaluated the bridge clearance algorithm on four bridges (three with known clearance problems). LiDAR-based measurements compare well with actually damage patterns on underside of bridges. LiDAR-based measurements were within +/- 5 cm of inventory clearance for the three bridges with known clearance issues. It is possible that the LiDAR measurements are more accurate than the inventory values.

Bridge defects: Liu et al. (2011) used terrestrial LiDAR together with the Light detection and range-based Bridge Evaluation (LiBE) system to detect defects in bridge structures. Liu et al. (2011) used a FARO LS 880HE phase-based scanner to generate a 3D model of a county bridge in North Carolina. The bridge was built in 1938 and is a reinforced concrete girder bridge with three 40-ft span. The bridge has large spalls underneath three of the four girders. The LiBE system was used to estimate the extent of spalling, and was able to detect that differential settlement of the bridge foundation was responsible for stress concentrations at the damaged locations.

Watson et al. (2011) used a terrestrial LiDAR scanner to evaluate blast damage to a culvert bridge. A single blast was conducted to remove a layer of rock for the construction of a sanitary sewer. The culvert was scanned prior to and after the blast to evaluate damage. A thorough comparison of the pre- and post-blast scans revealed no significant changes. Measurements were found to be within +/- 3.0 mm. Watson et al. (2011) suggest that LiDAR can be used to store 3D models of critical infrastructure for rapid evaluation of damage. According to the authors, it is much easier and faster to compare LiDAR point clouds or surface models constructed from LiDAR data than it is to evaluate photographs. It can be very difficult to identify the specific location of a photograph on a large bridge structure.

Drainage: Hans et al. (2003) performed a qualitative comparison of USGS 1/3 arc-second (~10m) DEM data with a 2-m DTM developed using airborne LiDAR. The stated accuracy of the LiDAR data was 15 cm RMSE. The analysis by (Hans et al. 2003) was strictly qualitative and compared the delineation of stream channels using both datasets. In general, the LiDAR-delineated streams more closely matched the actual stream location (as determined from aerial photography). The high resolution LiDAR data may actually increase processing time for drainage studies. In many cases, the LiDAR-generated surface must be modified to create a 'hydrologically correct' draingage network. For example, elevations at road crossings must be modified to lower the terrain to stream bed levels.

Shatnawi and Goodall (2010) studied flood top-width predictions from HEC-RAS for 10- to 500-year flood events on a 6.6-km stretch of river in the Piedmont area of North Carolina. They compared flood top-widths predicted using a) surveyed cross sections, b) LiDAR-derived cross sections, and c) hybrid data. The LiDAR data used were relatively coarse (20 ft grid cell size). In general, LiDAR-derived cross sections led to larger flood top-widths (larger inundated areas). The difference between LiDAR and conventional surveyed cross sections diminished as the return period increases (12% average difference for 10-year event, 4% difference for 500-year event). Shatnawi and Goodall (2010) noted that differences in surveyed and LiDAR cross sections were largest at locations immediately upstream or downstream of road crossings. This is likely due to the increased error noted by multiple studies (see section on LiDAR error sources below) in areas of steep and rapidly changing terrain. Higher flood top-widths with LiDAR data

could be attributed to the inability of the technology to penetrate water and detect the true bed elevation of the stream. The LiDAR DEMs might be excluding significant conveyance below the water level on the date LiDAR data were collected. Parr (2012) has developed a methodology for introducing channel conveyance below the surveyed waterline. This method requires surveyed cross sections to accurately describe the shape of the stream channel.

Straatsma and Baptist (2008) combined multispectral imagery with airborne LiDAR data to estimate vegetation height and density for use with the Delft3D-Flow hydrodynamic model. Height and density information were combined with drag coefficient to model the roughness of the vegetated area. The method was validated using the 2D-Horizontal mode in the Delft3D-Flow model, and was found to produce better hydrodynamic predictions as compared to traditional visual delineation of vegetation type and roughness parameters. Although the application of 2D hydrodynamic models is generally beyond the state of practice for highway drainage analysis, this work may lead to better methods for automatically updating river models for flood plain delineation.

Brook et al. (2010) investigated the use of LiDAR in conjunction with hyperspectral imagery to monitor civil structures. Hyperspectral imagery can be used to determine the chemical composition of urban materials (roof materials, pavement surfaces, etc.). Combined with LiDAR data, this can give a very detailed characterization of a watershed.

Pavement thickness: Walters et al. (2008) investigated whether LiDAR can be used to accurately assess pavement thickness to reduce the required number of cores. Coring is time consuming and requires a patch in the pavement that may be a future maintenance concern. Walters et al. (2008) used a terrestrial scanner (Leica Geosystems 3600) adjacent to the roadway. The general procedure includes a scan of the subbase prior to concrete placement, then a scan after the concrete has been placed and allowed to cure. This approach requires very precise and accurate georeferencing or site-specific tie points to allow the two scans to be compared. Walters et al. (2008) tested LiDAR-derived pavement thicknesses at three different locations, but did not make direct comparisons with cored data samples.

Rockfall hazards: Lato et al. (2009) used mobile terrestrial LiDAR to map three road and railroad segments in Ontario, Canada. MLS data were collected from a TITAN LiDAR system

mounted above a high-rail pickup truck. The TITAN system employs GPS and INS data to reference the location of the vehicle. Volumetric change detection was conducted by comparing multiple scans through time, allowing the detection of mass loss where rocks may have been released. The system effectively located areas of mass loss.

Road inventory studies: Pu et al. (2011) investigated the application of mobile LiDAR for conducting road inventory studies. The objective was to classify objects in the highway corridor based on automatic evaluation of a 3D point cloud. For example, signs might be inventoried based on the distinctive shape of the point cluster (e.g., octagon, rectangle, inverted triangle). At this point, the ability of the software is limited to the detection of poles and trees. Poles were detected with 86.9% success (verified with visual classification). Although this technology is promising for roadside inventories, it is in its infancy and will require significant development to reach production.

Zhou and Vosselman (2012) used aerial and mobile LiDAR point clouds to identify and map curbs for three test sites. Their detection algorithm focuses on finding the distinctive geometry of curbs in the point cloud. A verification analysis was conducted and found that the curbs were correctly identified with 90% correctness in the ALS and 89% in the MLS. ALS actually exhibited better performance, as the aerial LiDAR data are less affected by vehicles or other objects on the road. For the ALS data, curb location was identified with an RMSE of 11 cm. MLS positioning was more accurate (RMSE 6 cm), but was less complete due to obstructions at the road level. This technology could be very useful in planimetric mapping and in conducting automated road inventories. This study demonstrates that LiDAR can be used to identify break lines in topographic mapping, something that is often cited as a weakness of LiDAR data compared to other survey methods.

Vehicle classification/traffic flow estimation: Toth and Grejner-Brzezinska (2006) evaluated airborne LiDAR for remote sensing of traffic flows. The study used ALS data for a stretch of I-15 in Southern California. An Optech 3100 system was used to collect a LiDAR point cloud with 4 - 5 pts/m^2. The LiDAR scan was detailed enough to preserve the 3D shape of the vehicles, allowing accurate identification of vehicle class. This technology is unproven and in early stages of development.

Urban mapping: Hinks et al. (2009) developed a flight planning strategy to optimize mapping in urban areas. When mapping buildings, it is critical to collect detailed scans of the vertical surfaces. Hinks et al. (2009) conducted a case study using the flight planning approach for the city of Dublin, Ireland. They conclude that carefully planned, multiple overlapping flight paths that are diagonal to the main orientation of streets generate a level of detail much higher than previously achieved.

Streambank retreat monitoring: Resop and Hession (2010) studied streambank retreat using a terrestrial LiDAR scanner. A streambank section of Stroubles Creek in Blacksburg, Virginia, was surveyed six times in two years using both TLS and traditional, total station measurements. Streambank retreat rate was estimated at -0.15 m/yr using TLS and -0.18 m/yr using total station. Resop and Hession (2010) compared LiDAR measurements to surveyed cross sections. Although error is present in the LiDAR point cloud, total station data requires interpolation between sparse surveyed points. The magnitude of this interpolation-based error is often not recognized or assessed in evaluations of LiDAR data.

Bathymetric mapping: Bailly et al. (2010) performed a rigorous geostatistical evaluation of bathymetric LiDAR data for rivers. Bathymetric mapping is accomplished using two laser wavelengths. In this case, a Hawkeye II LiDAR system was employed, using a wavelength of 1064 nm (near-infrared) to detect ground and water surface elevations and a wavelength of 532 nm (green) was used to map the stream bathymetry. Their study focused on a 1.5 km stretch of a shallow, gravel-bed stream in southern France. Bailly et al. (2010) compared the LiDAR data to a detailed GPS survey of the stream. The LiDAR data had a random error standard deviation of 32 cm. The lower limit of depth detection for rivers using current technology is approximately 50 cm; gravel streams are often shallow and may not be suitable for LiDAR-based bathymetric mapping. Hilldale and Raff (2008) suggest that LiDAR-generated bathymetric models area suitable for mesoscale mapping of riverbed landforms for habitat analysis. However, LiDAR bathymetric mapping must be improved before it can be used for hydraulic studies of small areas.

Mapping sinkholes: Carter et al. (2001) note that sinkholes are difficult to detect using traditional photogrammetric methods in heavily-vegetated areas. LiDAR penetration of the

canopy is able to identify sinkholes with much greater reliability and may prove invaluable for detecting subsidence in areas adjacent to highways or along proposed highway corridors.

Pipeline mapping: Tao and Hu (2002) evaluated the use of LiDAR for pipeline risk management. LiDAR is particularly well-suited for corridor mapping (aircraft can follow the pipeline or road corridor). LiDAR data may be used to identify areas of steep slopes that may be a concern for pipe sections that may be at risk of ground displacement or fire damage. This study is qualitative in nature and presents a very good summary of LiDAR technology and characteristics.

Forest succession: Falkowski et al. (2009) used aerial LiDAR collected at an elevation of 2500 m. The vertical RMSE of resulting DEM was 30.6 cm in areas of high canopy cover and 16.6 cm in low canopy cover areas. LiDAR returns at multiple levels (top of canopy and ground level) were used to classify the successional stage of the forest with over 90% accuracy.

2.3 Error Quantification

It is difficult to make general statements regarding the accuracy of LiDAR data. The error analysis in this section focuses primarily on ALS; few published studies have documented the errors associated with TLS or MLS.

2.3.1 Sources of Error

There are multiple sources of error in airborne LiDAR estimates. The nature and superposition of these errors has made it difficult to improve the vertical accuracy of ALS surveys beyond 15 cm RMSE (Baltsavias 1999), though a few very recent studies have achieved vertical RMSE < 10 cm.

Huising and Pereira (1998) provide a detailed description of the sources and magnitudes of errors associated with laser scanners. In general, the major sources of error can be categorized as laser, location, terrain / vegetation, and post-processing errors (Al-Durgham et al. 2010; Huising and Pereira 1998). A brief description of each error type is provided here.

1. Laser error: Laser error can be broken into two major categories: range uncertainty and angle error (Glennie 2007). Range uncertainty is a function of the LiDAR type (range- or phase-

based), laser wavelength, and the sensitivity of the LiDAR unit (the internal clock used to measure the timing of the return). Most airborne LiDAR manufactures quote a range uncertainty on the order of 1 to 3 cm (Glennie 2007; Tao and Hu 2002).

Laser angle error is a function of the angular resolution of the LiDAR unit and beam divergence. The angular resolution is dictated by the mechanical precision of the LiDAR mirror system. Atmospheric beam divergence causes the laser footprint to expand with distance from the LiDAR unit. Although the laser pulse is emitted as essentially a point of light, by the time the laser pulse hits the ground it has generally spread to a footprint that is 24 to 60 cm wide (Hodgson and Bresnahan 2004). Beam divergence results in uncertainty in the x, y location of the portion of the ground that actually contributes to the laser return. Angle uncertainty in LiDAR measurements lead to larger uncertainty in the x, y position than in the vertical component of observed point locations.

The vertical accuracy of the LiDAR elevation decreases with laser attitude (angle of the laser pulse relative to a straight line drawn from the aircraft to the ground) (Baltsavias 1999). This is due in part to the increased distance between the aircraft and the ground (greater range error, greater beam divergence).

2. Location: The aircraft GPS plus inertial navitation system (INS) system has a vertical accuracy on the order of 5 - 7 cm. Although improvements in GPS and INS technology may reduce this error in time, it is currently a major contribution to the error budget of ALS data. One infrequently-noted source of error in this system is due to the lever-arm offset, or the offset between the center of observations from the laser scanner and the center of the navigation susbsystem. An accurate measurement of this offset and the relative alignment of the two systems is critical for improving the accuracy of ALS and MLS surveys (Glennie 2007).

3. Terrain/vegetation: LiDAR accuracy degrades with increasing ground slope and increasing vegetative cover. The ground slope affects LiDAR accuracy because of the relatively large horizontal error associated with LiDAR (horizontal RMSE can be over 50 or 100 cm). In steeply sloped areas, an error in horizontal position of a ground point contributes to error in the vertical position. For example, if the ground is sloped 30%, a 100 cm error in the horizontal

would contribute to a 30 cm error in the vertical. This means that LiDAR accuracy is degraded for ditches, stream channels, levees, and road embankments.

Dense vegetation limits the penetration of laser pulses to the ground. This can be compensated for by multiple fly-overs, lower flight elevations, increased overlap between swaths, and improvements in post processing.

Water generally absorbs the laser signal, but can cause a data reflection (particularly at a low angle of incidence). Asphalt can absorb the laser signal in some cases. This was noted by (Huising and Pereira 1998) for an ALTM laser system using a wavelength of 1.047 μm.

4. Processing: Automated filtering of LiDAR data to remove vegetation and develop bare-earth DEMS can be incomplete and/or can cause real ground returns to be removed from the dataset. Careful post processing is just as important as careful planning and execution of the LiDAR data collection effort.

2.3.2 Documented Errors

Baltsavias (1999) points out that the errors stated by LiDAR service providers tend to be optimistic. Although the consensus among service providers seems to be a vertical RMSE of 15 cm (Veneziano et al. 2004), multiple factors affect the total error budget. As seen in the previous section, Glennie (2007) provides a theoretical model for errors contributing to ALS uncertainty. This section evaluates the published literature on ALS error comparisons with photogrammetric and conventional real-time kinetic global positioning system (RTK-GPS) and/or total station ground survey results. The research papers and reports are cited in chronological order. Table 2.1 summarizes the error analyses for ALS surveys.

Ultimately, ALS elevation mapping is in direct competition with digital or softcopy photogrammetry. Baltsavias (1999) provides a detailed comparison of the errors, advantages, and disadvantages of ALS relative to photogrammetry. Baltsavias (1999) states that ALS has a constant error of 5-20 cm (due mostly to GPS and ranging), with an additional error of 0.5-2 cm per 100 m of elevation above ground level. By contrast, photogrammetry has a constant error term of approximately 2-5 cm plus an additional error of 1.6 cm per 100 m of aircraft elevation AGL (Baltsavias 1999). For a flying height of 400 – 1000 m, photogrammetry is expected to

have slightly lower error than ALS. However, in good conditions ALS elevation estimates can be more accurate than photogrammetric estimates. ALS is expected to perform better relative to photogrammetry for higher flying elevations (Baltsavias 1999). One large advantage of ALS compared to photogrammetry is the degree of automation in processing final maps, which greatly increases the speed of delivery. However, the automated filtering agorithms (which distinguish vegetation and building returns from ground returns) tend to smooth out some terrain features (Baltsavias 1999).

Pereira and Janssen (1999) evaluated ALS for generation of DTMs for use in highway planning. Their study investigated the altimetric and planimetric accuracy of the ALS raw laser measurements and of the final 1 m x 1 m LiDAR-generated DTM. The ALS was conducted using a low-flying helicopter-based system with a point density of 4 points per m^2. ALS data were compared to a) total station elevation measurements and b) planimetric estimates. It should be noted that the accuracy of the planimetric maps used was assumed but not known. Raw laser altimetric measurements had a mean error of -5 cm for bare soil and -2 cm for low grass. The RMSE for the raw laser measurements was found to be 10 cm for bare soil and 16 cm for low grass. The laser-based DTM was compared to a photogrammetry-based DTM. For flat terrain, the laser-based DTM vertical RMSE ranged from 8 cm to 15 cm. For sloped terrain, the vertical RMSE increased to 25-38 cm. The overall mean vertical RMSE was 29 cm. Pereira and Janssen (1999) point out that the accuracy of photogrammetry-based DTMs is often assumed and not rigorously determined. It appears that the accuracy of LiDAR survey data has received more scrutiny than photogrammetric methods.

Cowen et al. (2000) studied the application of ALS to a rail construction econometric model. LiDAR data were collected using a helicopter-mounted system. The helicopter flew at approximately 228 m AGL at a forward air speed of 25 m/sec. Analysis of the LiDAR returns found that 80-90 percent of pulses reached the ground when the vegetative canopy cover was 30-40 percent. In areas of denser vegetation (80 to 90 percent) only 10 to 40 percent of pulses reached the ground. Cowen et al. (2000) compared the LiDAR-generated DTM with surveyed elevations and found an error of +/- 50 cm. The article does not specify whether this error is the RMSE or +/- one standard deviation.

Brinkman and O'Neill (2000) suggest that vertical accuracies of 7 to 8 cm are possible if flight layouts are carefully planned to optimize GPS positioning of the aircraft. Given that GPS uncertainty is a significant contributor to the overall error budget, it makes sense to plan ALS surveys to maximize the availability of GPS satellite information.

Uddin (2002) collected LiDAR data for direct comparison with aerial photogrammetry-derived contours and ground-based topographic survey (total station) results. All survey data were acquired within several months of each other. LiDAR data were processed in CAD to generate 1-ft contours of the survey site. Uddin (2002) determined that the vertical RMSE between total station and LiDAR data was 15 to 18 cm, depending on vegetation. Uddin (2002) points out that the LiDAR survey cost approximately one-half as much as the traditional ground survey. Although the LiDAR RMSE is relatively high, the density of points is much higher. Traditional ground surveys require interpolation methods to estimate elevations between surveyed points. LiDAR point density is high enough to vastly reduce the degree of uncertainty introduced through interpolation. Uddin (2002) found that LiDAR, photogrammetry, and total station mean elevation data were not statistically significant from each other at a 95% confidence level. Uddin (2002) suggests that ALS is capable of producing a DEM with spatial resolution up to 15 cm and vertical accuracy to 15 cm. These characteristics make ALS data suitable for the generation of 1 ft contours (Uddin 2002).

O'Hara (2002) evaluated the use of LiDAR and hyperspectral aerial imagery for classification and mapping of wetlands in the Deep River watershed in North Carolina. O'Hara (2002) developed a classification strategy that included hydrologic and vegetative assessments; they compared their findings with existing wetland inventories and found very good agreement (95%). Early collection of aerial LiDAR data and imagery may be useful in preliminary assessment of wetlands for new highway construction or realignment projects (O'Hara 2002).

Adams and Chandler (2002) studied airborne LiDAR accuracy for a coastal mudslide study and found a RMSE of 26 cm. It should be noted that the LiDAR survey was compared to photogrammetric elevations. The error characteristics of the photogrammetric elevations are not known. Overall, the LiDAR map was found to be less sensitive to slope than the digital photogrammetry.

Bowen and Waltermire (2002) evaluated LiDAR accuracy for elevation mapping along a western river corridor. The overall accuracy of the LiDAR elevations was 43 cm (RMSE). Bowen and Waltermire (2002) found that algorithms to remove vegetation signals in the LiDAR data were far less effective in locations of steep slope.

Veneziano et al. (2002) performed a thorough analysis of error and compared LiDAR-generated DTMs to photogrammetric elevations. GPS-surveyed elevations were used for the control. The LiDAR data were interpolated using two methods (TIN and IDW). Using the 1-m TIN-generated DTM, the RMSE for LiDAR was 33 cm for hard surfaces, compared to 17 cm for the photogrammetric elevation map. For ditches, the LiDAR RMSE was 60 cm while the photogrammetric RMSE was 52 cm.

Hodgson and Bresnahan (2004) conducted a thorough study of airborne LiDAR accuracy using a dataset collected from an elevation of 1207 m AGL with a 2-m posting. They compared the LiDAR data with total station and rapid-static GPS measurements. The RMSE for the LiDAR data ranged from 17.2 cm for evergreen forest, 18.9 cm for pavement, and up to 25.9 cm for deciduous forest. The elevation RMSE in locations of steeper slopes (> 25 degrees) was double that in flatter areas.

Veneziano et al. (2004) compared ALS mapping with Electronic Distance Measurement (EDM), Real Time Kinetic Global Positioning System (RTK-GPS), and photogrammetry. Their study found that LiDAR accuracy depends on surface condition. The RMSE values for hard surfaces was 32 cm for LiDAR compared to 16 cm for the photogrammetry-derived surface. Error increased for both data collection methods for ditches and steep slopes, with LiDAR RMSE approximately 2x photogrammetry-derived RMSE in all cases. Veneziano et al. (2004) ecommend that LiDAR be used for general terrain mapping where accuracy is not of utmost importance.

In addition to developing a theoretical error model of LiDAR accuracy, Glennie (2007) tested fixed-wing, helicopter, and mobile LiDAR platforms. The fixed-wing field verification flight (conducted at 1000 m AGL with a 1 m data posting) had a vertical RMSE of 8.6 cm and a horizontal RMSE of 61.8 cm. The helicopter-based test survey was flown at 100 m AGL. The vertical RMSE was determined to be 8.9 cm and the horizontal RMSE was 29.2 cm. The mobile

LiDAR system was vehicle-mounted. The RMSE for the ground-based LiDAR was 5.9 cm; the majority of this error was due to the range uncertainty of the LiDAR unit. Glennie (2007) used a worst-case laser orientation for this study, so the stated RMSE for the mobile LiDAR application may be conservative for most applications.

Paska and Ray (2007) present an analysis of the airborne LiDAR system acquired by the Ohio DOT in 2004 (an Optech ALTM 30/70). Their paper analyzes how various data collection and processing decisions affect the accuracy of a final TIN. The factors which affect the accuracy of the LiDAR elevation mapping are: "flying height, aircraft velocity, scan angle, scan frequency and pulse frequency" (Paska and Ray 2007). Distance to the nearest Continuously Operated Reference Station (CORS) also affects data accuracy. Paska and Ray (2007) determined the impact of distance to CORS and Positional Dilution of Precision (PDOP), a measure of the quality of the GPS satellite fix, on accuracy in the final TIN. Mean vertical error ranged from just under 4 cm for very good satellite fix (PDOP = 1.2) up to 14 cm for PDOP approaching 5. Error increased rapidly with distance from CORS (0 cm to 11.2 cm as the project site moved from 0 km to 120 km from CORS station).

Al-Durgham et al. (2010) compared airborne LiDAR data in an urban area of Ottawa, Canada with two GPS datasets. The total study area consisted of 22 strips over 6 km^2. The average point spacing was 30 cm. An RTK-GPS system was used to collect 45 validation points. The other GPS dataset was collected using a GPS in a moving vehicle. It is interesting to note that there was a systematic difference of (on average) 7.9 cm between the two GPS datasets, even though the stated accuracy of the RTK-GPS system was 2 cm and the vehicle-mounted GPS reported a vertical accuracy of +/- 4 cm.

Skaloud et al. (2010) published a methodology for geo-registration of ALS data in flight. The approach integrates GPS, IMU, and LiDAR data. Their approach focuses on the use of RTK-GPS positioning of the aircraft. This requires in-flight communication with GPS base stations for real-time registration. Skaloud et al. (2010) used a flight height of 250 m and collected an average of six points per square meter to test the methodology. This technology is still unproven, but indicates that the errors in ALS can be reduced with improvements in technology.

Vincent and Ecker (2010) compared ALS survey data to convential survey control points for the Missouri DOT. Their study found a vertical RMSE of 5.27 cm. The ALS survey collected 15 pts/m^2 using a flight elevation of 500 m and an average airspeed of 100 knots. The projected vertical accuracy was 8 cm, so actual performance exceeded expectations.

Only two reports were found that documented MLS accuracy. Lato et al. (2009) discuss the use of a high-rail truck to perform LiDAR data collection along a 20 km stretch of rail in Ontario, Canada. Much of the railroad is in a narrow canyon, limiting GPS signal availability. Much of this is overcome through the use of an INS. Global accuracy of the data collected was +/- 15 cm. Vincent and Ecker (2010) compared MLS survey data to conventional survey control data. Their analysis found a vertical RMSE of 3.84 cm.

Only one report was found that documented TLS accuracy. Bethel et al. (2005) conducted a thorough analysis of error in a TLS survey of two bridges over the I-70 corridor in Indiana. LiDAR scans were compared with traditional survey data provided by the Indiana DOT. The maximum discrepancies between LiDAR and the traditional survey data were 3.85 cm in the horizontal and 1.52 cm in the vertical. The entire data collection effort was completed in two days for both bridges. The authors determined that the LiDAR survey produced the same level of accuracy as conventional survey methods, but in a time and cost-effective manner.

TABLE 2.1
Summary of Error for Aerial LiDAR Elevation Surveys

Application	Vegetation	Vertical Accuracy (cm RMSE)	Citation
Highway Mapping	Leaf-Off	6 to 10 (roadway)	(Shrestha et al. 1997)
Costal, River Management	Leaf-Off	18 to 22 (beaches) 40 to 61 (sand dunes) 7 (flat and sloped, low grass)	(Huising and Pereira 1998)
High slopes, rough terrain		50-100 cm	(Kraus and Pfeifer 1998)
Road Planning	Leaf-Off	8 (lines on roads) 25 to 38 (sloped)	(Pereira and Janssen 1999)
Flood Zone Management	Leaf-Off	7 to 14 (flat areas)	(Pereira and Wicherson 1999)
Archeological Mapping	Leaf-Off	8 to 22 (prairie grassland)	(Wolf et al. 2000)
Highway Engineering	Leaf-On	3 to 100 (flat grass areas, ditches, rock cuts)	(Berg and Ferguson 2000)
Rail planning	Leaf on	50 cm	(Cowen et al. 2000)
	Leaf on		(Cobby et al. 2001)
Coastal mudslide study		26 cm	(Adams and Chandler 2002)
River corridor mapping		43 cm	(Bowen and Waltermire 2002)
	Leaf on	33 cm (low grass) 153 cm (scrub / shrub)	(Hodgson et al. 2003)
Highway Corridor Mapping	Mixed	32 (for 2-m DEM, hard surfaces) 70 (ditches) 44 (steep slopes) 20 (bare surfaces)	(Veneziano et al. 2004)
Research		18.9 (pavement) 22.5 (low grass) 18.9 (high grass) 23.3 (brush / low trees) 17.2 (evergreen) 25.9 (deciduous)	(Hodgson and Bresnahan 2004)
Coastal Mapping, 5 m DEM		15.5 cm (95% RMSE)	www.ncfloodmaps.com, as cited by (Hodgson and Bresnahan 2004)

TABLE 2.1 (continued)
Summary of Error for Aerial LiDAR Elevation Surveys

Application	Vegetation	Vertical Accuracy (cm RMSE)	Citation
Airport site		8.6 (airport)	(Glennie 2007)
Forestry mapping	Leaf on	30.6 cm high canopy 16.6 cm low canopy	(Evans and Hudak 2007)
Forest succession	Leaf on	30.6 cm (high canopy cover) 16.6 cm (low canopy cover)	(Falkowski et al. 2009)
	Mixed Landuse	2 to 6	(Al-Durgham et al. 2010)
Highway mapping		5.27	(Vincent and Ecker 2010)

Chapter 3: KU CEAE Experience with LiDAR

3.1 Description of KU Riegl System

In 2008, the University of Kansas Kansas Geological Survey, Department of Geology, and Transportation Research Institute purchased a Riegl LMS-Z620 terrestrial laser scanner. This scanner has a maximum range, under ideal conditions, of 2 km. The stated ranging accuracy of the laser is 10 mm. The Riegl LMS-Z620 uses a Class 1 near-infrared laser and is capable of collecting 11,000 points per second. This chapter describes three applications of the TLS.

3.2 Research Conducted with KU's System

3.2.1 Stream Corridor Mapping

This section contains text and figures from (Young 2011), an unpublished report to the Kansas Water Office.

The Kansas Water Office (KWO) funded a large stream restoration and stabilization project on the Neosho River west of Neosho Rapids, Kansas. The restoration project involves work on twelve 'Hot Spots' along an 8.3 mile stretch of the river (Figure 3.1). The objective of this study was to document as-built topography for the twelve hot spots using a terrestrial laser scanner (TLS).

All twelve hotspots were scanned using the Riegl LMS-Z620 laser scanner owned and operated by the University of Kansas. The Riegl scanner has a maximum range of 2 km and has a rated accuracy of 10 mm for a single scan collected from a stationary position. The Riegl scanner employs a Class 1 laser using a near-infrared wavelength. The scanner collects 11,000 points per second. Figures 3.2 and 3.3 show the Riegl scanner setup.

Each streambank restoration site required multiple scanner set-ups in order to capture the topography of both the inner and outer streambank. In general, the scanner was set up along the top of the streambank near the ends of each construction site. For most sites, one or two additional locations were selected along the stream bank to ensure full coverage.

Multiple scans are joined together by means of reference points in each scan. These reference points are usually established by setting up reflective tie points on tripods across the study area. A minimum of four tie points are required to reference overlapping scans. For this

study, a minimum of six tie points were set up at each streambank site. For most locations, reflective cylinders (10 cm diameter radius, 10 cm tall) were used for tie points. These tie points were set up on tripods. Figure 3.4 shows a tie point reflector mounted on double range poles at site 25. Single range poles were used at all other locations.

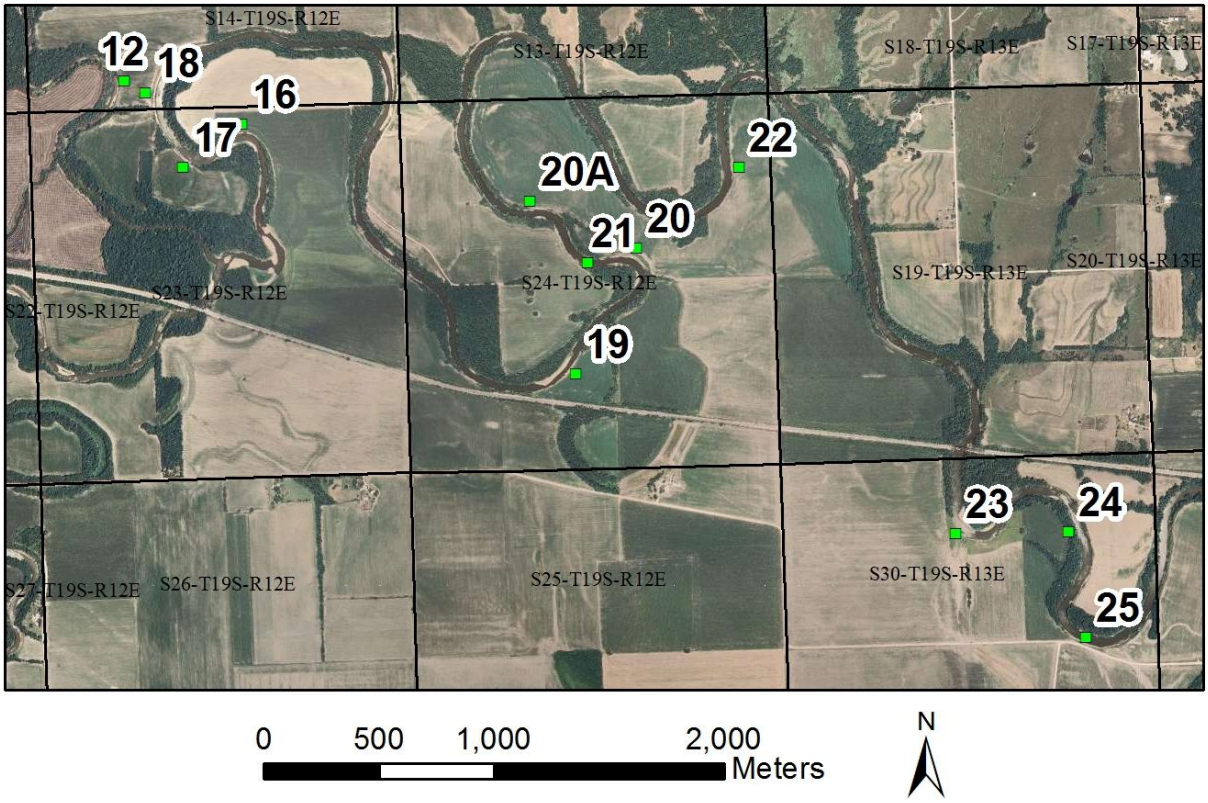

FIGURE 3.1
Location of the Twelve Hot Spots along the Neosho and Cottonwood Rivers

For sites requiring more than eight tie points, reflective cylinders were set up on hay bales or on the ground. Reflective prisms were used in addition to the cylindrical tie points at sites 17, 18, 23, and 25. Extra caution must be employed when using the reflective prisms, as the strength of the laser return can damage the Riegl TLS if it is setup within 100 m of the prism.

Scans of each site were georeferenced using Global Positioning System (GPS) equipment to observe real-earth coordinates for at least four tie points per site. A Trimble 5800 Real Time Kinetic GPS (RTK-GPS) unit owned by the University of Kansas Department of Geology was used to georeference tie point locations for sites 17, 18, 23, and 25. At these sites, the base

station was set up for at least 20 minutes prior to beginning the survey to improve survey accuracy. For all other sites, static GPS receivers (TOPCON GB-1000) were mounted on top of four tie point reflectors to collect x, y, z coordinates and were left in the field for the duration of the survey (typically more than one hour per site).

FIGURE 3.2
The Riegl LMS-Z620 Terrestrial Laser Scanner at Site 25

FIGURE 3.3
The Riegl System at Site 25, Including Generator and Laptop. Tiepoints Are Visible to the Right of the Scanner (on the Terrace) and in the Distance at the End of the Project

FIGURE 3.4
Leveling a 10 cm Reflective Tie Point The Photograph Shows the Tie Point Mounted on Double Range Poles. Single Range Poles Were Adequate for All Sites in This Study.

LiDAR point clouds were developed for each scanning position. Typically, the scanner was set up to collect approximately two million data points per scanner position. Overlapping scans were merged and georeferenced using Riegl software (RiScan Pro 1.5.5). Figures 3.5, 3.6, 3.7, and 3.8 illustrate the assimilation of multiple scans for site 22. Figure 3.9 shows the LiDAR point cloud from scan position 4. Laser ‘shadows’ can be seen behind the hay bales.

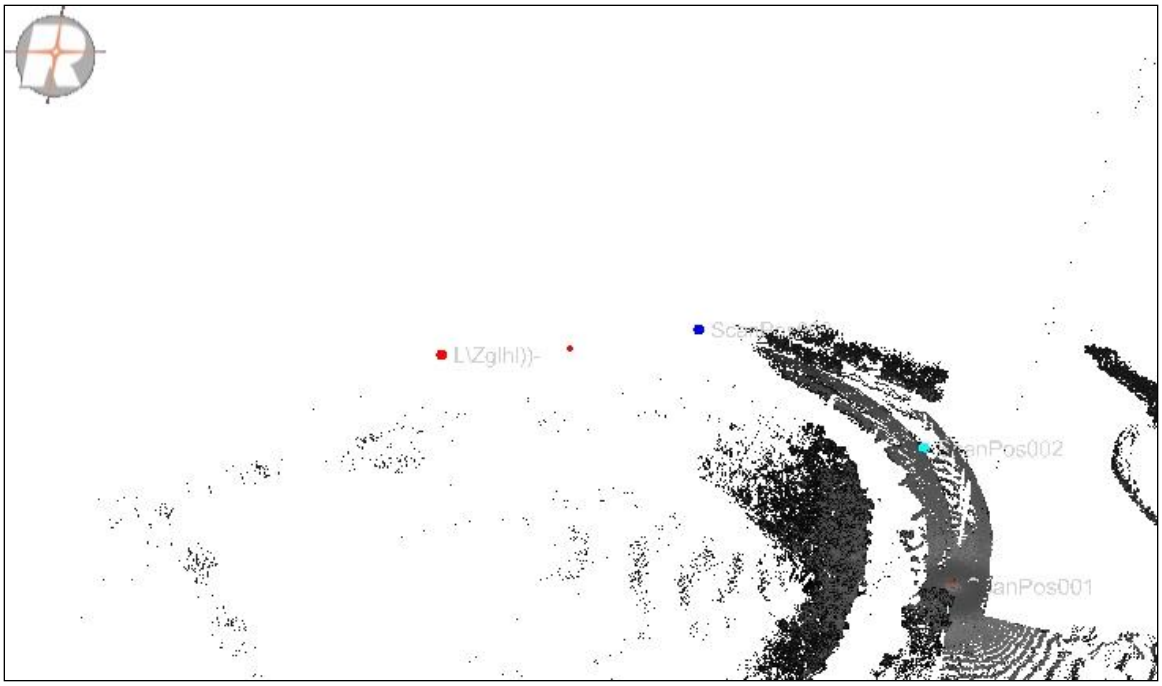

FIGURE 3.5
LiDAR Points for Site 22, LiDAR Position 1

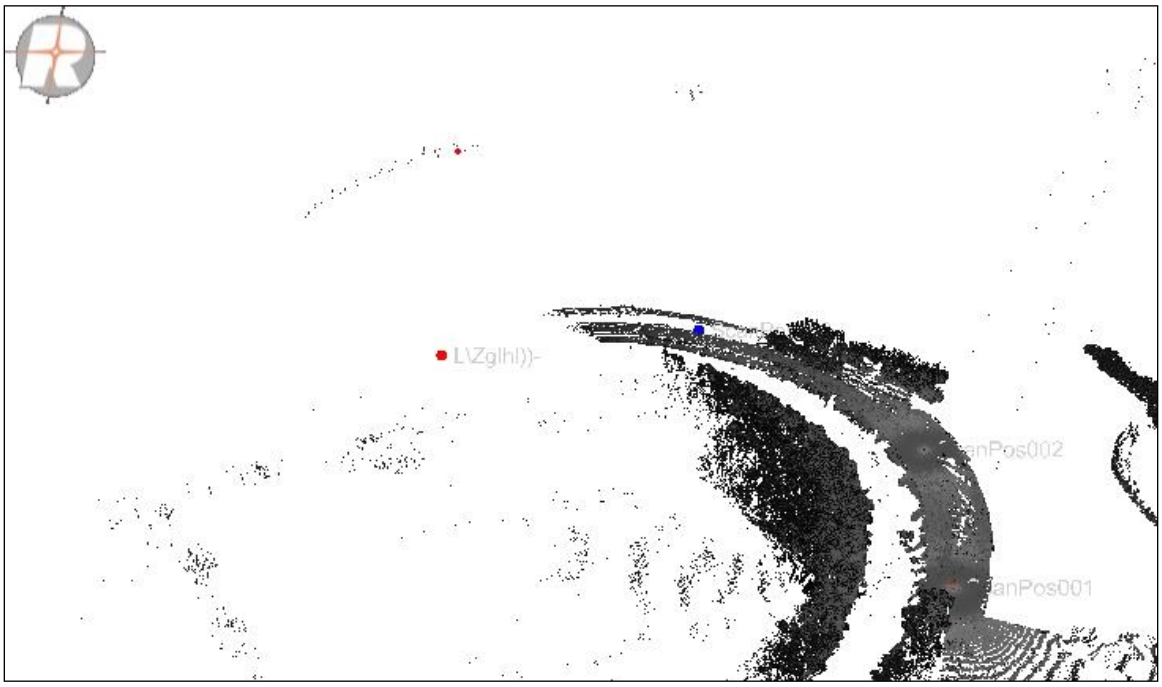

FIGURE 3.6
LiDAR Points for Site 22, LiDAR Positions 1 and 2

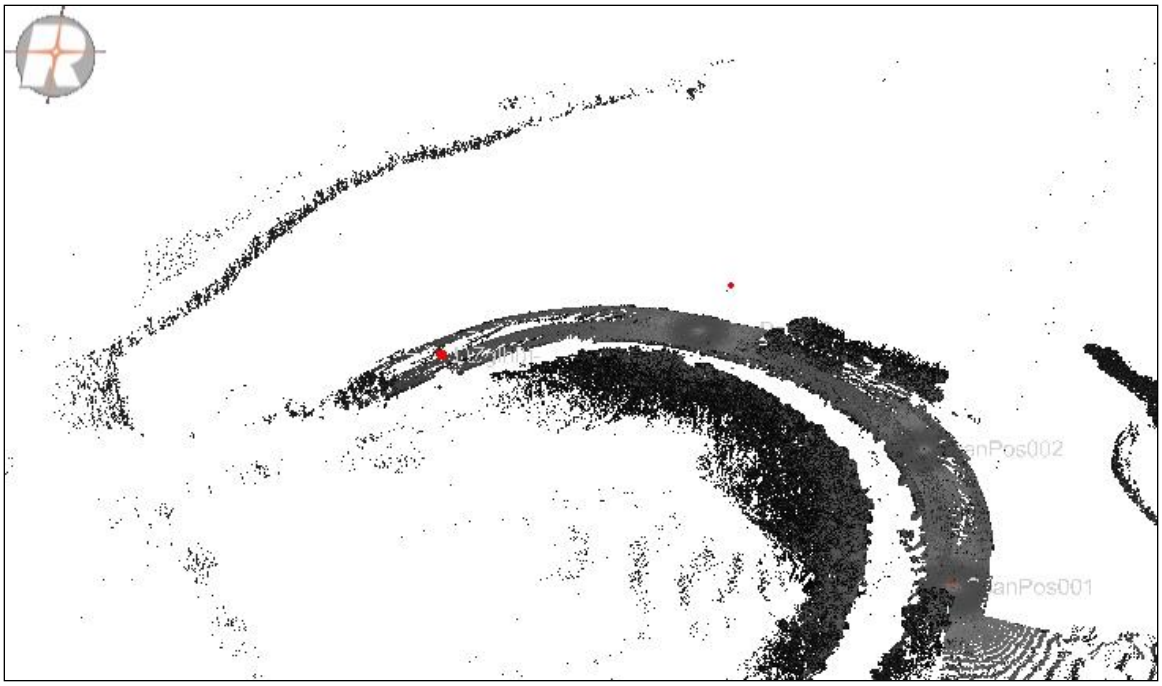

FIGURE 3.7
LiDAR Points for Site 22, LiDAR Positions 1, 2, and 3

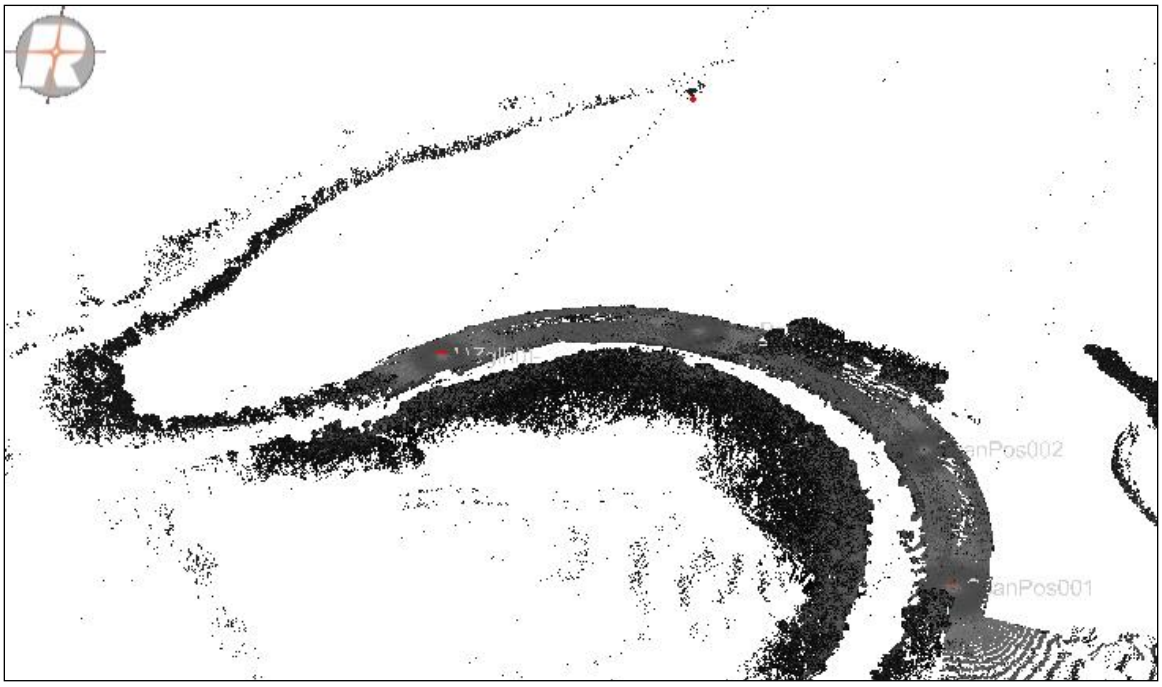

FIGURE 3.8
LiDAR Points for Site 22, LiDAR Positions 1, 2, 3, and 4

FIGURE 3.9
LiDAR Points for Site 22, LiDAR Position 4

TerraScan (a third party plugin to MicroStation, developed by TerraSolid) was used to post-process the LiDAR point clouds in order to remove vegetative returns and other data errors. One unanticipated error was caused by the laser reflecting off of the river surface and returning a mirror image of the vegetation on the bank. These returns must be manually identified and removed from the point cloud.

ArcGIS software was used to generate TINs and DEMs from the LiDAR point cloud data. The final DEMs were generated using a 10 cm cell size. Smaller DEMs can be generated from the TINs if required for future analysis.

All final GIS deliverables were referenced to UTM Zone 14N using the North American Datum of 1983. Vertical coordinates are referenced to the NAVD88 vertical datum.

The project deliverables to KWO included raw and final LiDAR pointclouds, TINs, and 10-cm DEMs for all twelve surveyed sites. In addition, historical aerial photographs were collected and, where necessary, georeferenced for 1938, 1957, 1976, 1991, 2002, and 2006. Figure 3.10 shows the 2006 aerial photograph of Site 19. Figures 3.11 and 3.12 show the LiDAR-generated TIN and DEM for the same site. These examples illustrate the data deliverables.

FIGURE 3.10
2006 Aerial Photograph of Site 19

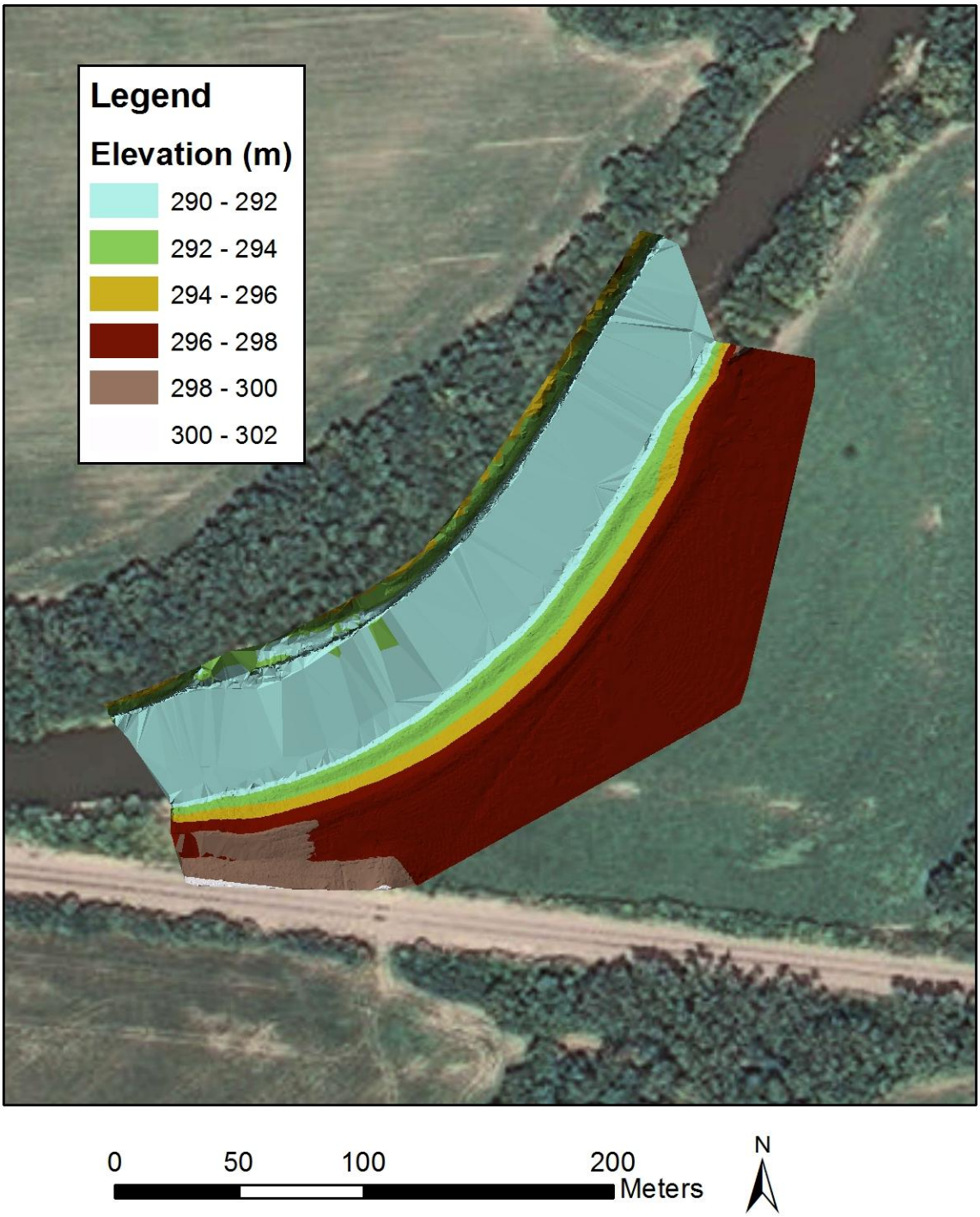

FIGURE 3.11
LiDAR-Generated TIN of Site 19

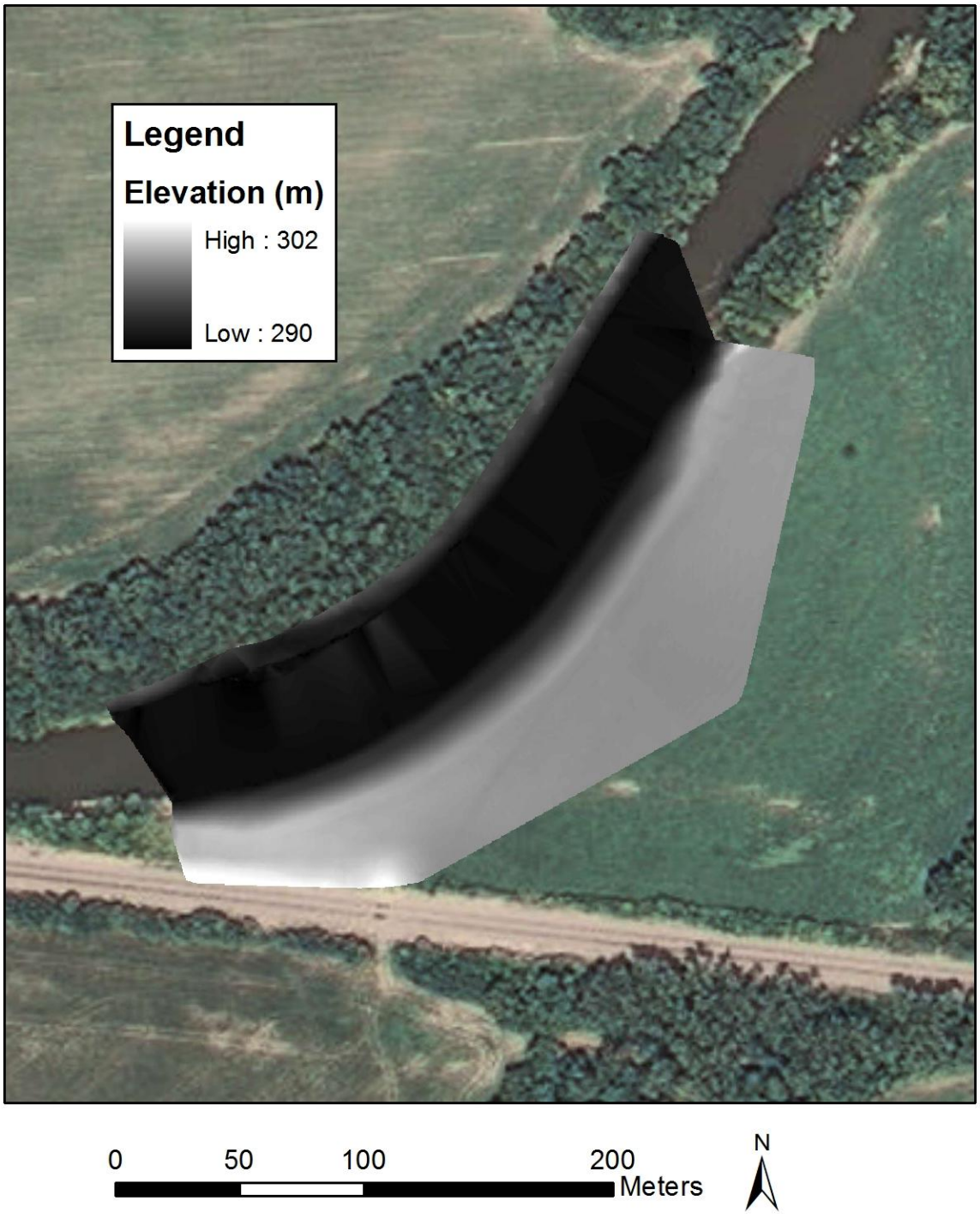

FIGURE 3.12
LiDAR-Generated 10-cm DEM of Site 19

Based on the density of vegetation adjacent to the streambank restoration sites, and based on the planting strategy selected for the restorations, it will be challenging to re-scan the sites using a terrestrial scanner. Aerial Laser Scanning (ALS) might be employed to develop DEMs of the sites in the future. However, ALS is currently limited to a typical vertical accuracy of approximately 15 cm RMSE and may not be sufficient to map out mass loss (or gain) along the streambanks. Careful planning and execution of the ALS survey may achieve accuracy < 10 cm, which may be suitable for evaluating large changes to the streambanks.

If TLS is used to scan the sites in the future, it is recommended that the scanning equipment be deployed on the inner bank of each meander, with 360-degree prisms used for tie points along the outer bank. Dual access to both the inner and outer bank will increase project cost and timing. If multiple future scans are planned, absolute survey benchmarks (with State Plane coordinates and vertical datum) should be established for each site to improve georeferencing of LiDAR survey data.

3.2.2 Highway Subsidence Study

Herrs (2010) used the Riegl LMS-Z260 to study subsidence along US Highway 50 in Reno County, Kansas. LiDAR surveys were conducted for the Brandy Lake and Victoria Road sinkholes. The resolution of LiDAR data ranged from 10 points/m^2 at a range of 500 m to over 500 points/m^2 at a range of 2 m from the LiDAR unit. The Trimble 5800 RTK-GPS was used to georeference the locations of tie points for the study. Five scanner locations were used for the Victoria Road sinkhole, while six separate locations were used for the Brandy Lake location.

Six surveys were conducted at the two locations over the period October 2008 – February 2010. Scans were analyzed for changes; no changes were detected during the period of study within the detection capability of the TLS scans. Error estimated for the scans is between 3 – 6 cm vertical RMSE, which may mask small changes between successive scan dates. MLS may have been an appropriate alternative for this application, given similar error characteristics and the level of effort required to scan long, linear features with TLS.

3.2.3 Deformation Study of Steel-Reinforced Pipe

Khatri et al. (2012) used the KU Riegl LMS-Z260 scanner to supplement data collection during deformation tests of a steel-reinforced high-density polyethelene pipe. A phase-shift laser scanner would be much more appropriate for this application, given the higher accuracy and faster data collection rate. The Riegl scanner used conducted a full scan of the pipe over a period of approximately 30 seconds. This collection rate was not adequate given the rate of deformation of the pipe during the period of the test. The LiDAR data provided qualitative 3D imagery of the pipe at various stages of deformation. Figures 3.13 and 3.14 show before and after scans. Keep in mind that these are 3D scans shown from only one perspective. The advantage of a LiDAR scan as opposed to photography in this case is that the 3D pipe section can be viewed from multiple angles.

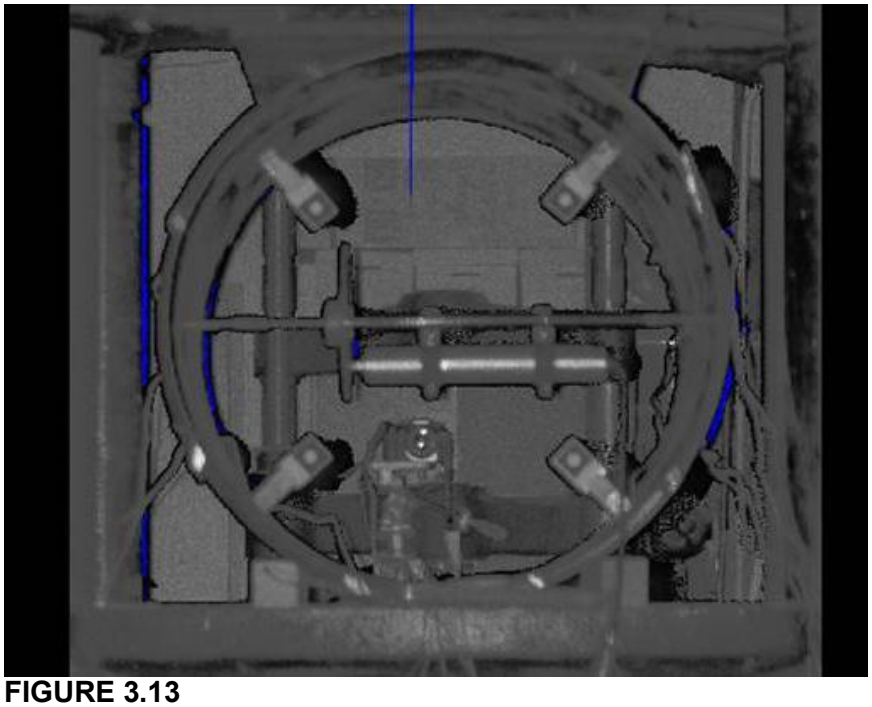

FIGURE 3.13
LiDAR Scan of the Pipe Prior to the Test

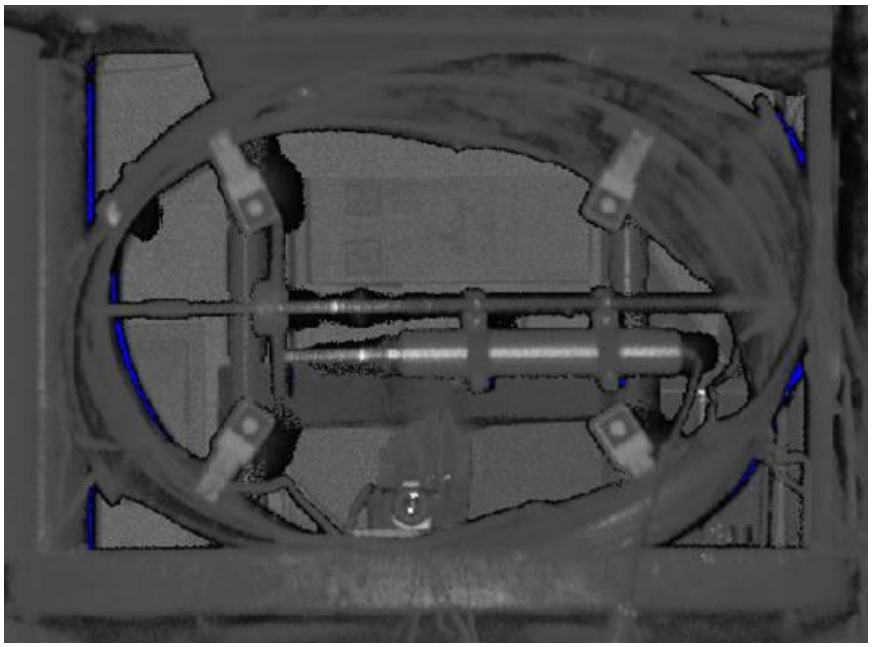

FIGURE 3.14
LiDAR Scan of the Pipe after Testing

Chapter 4: LiDAR Data Available in Kansas

4.1 LiDAR Data in Kansas

The Kansas Data Access and Support Center (DASC, www.kansasgis.org) maintains a collection of publically available GIS data for the State of Kansas. This resource includes county-wide ALS-generated DEMs for much of the State. LiDAR mapping has been conducted in four years: 2006, 2009, 2010, and 2011. Figure 4.1 shows the counties covered in each survey series. LiDAR surveys are underway and planned for many other counties at the time of this report.

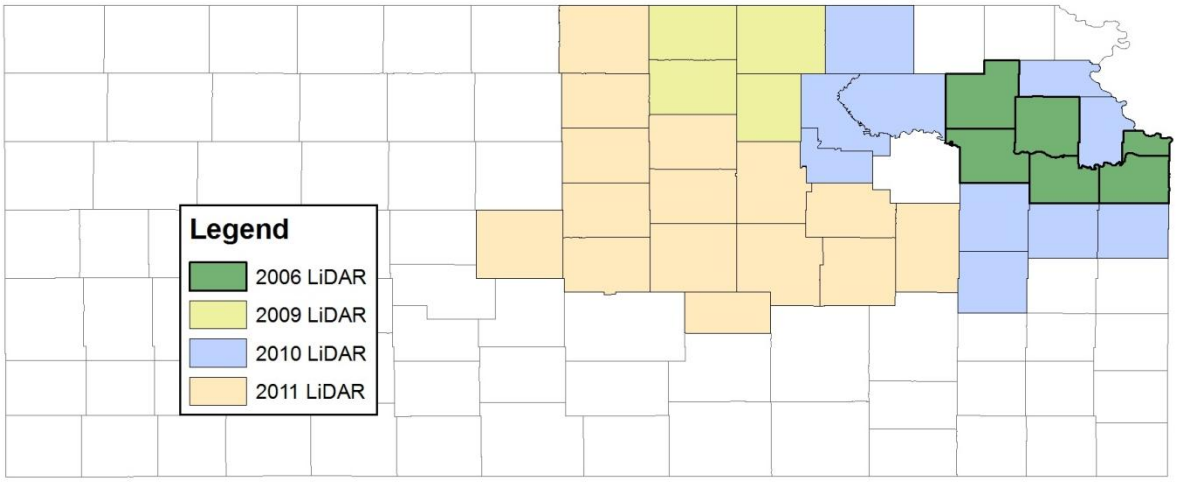

FIGURE 4.1
Status Map for LiDAR Surveys Conducted in Kansas

The positional accuracy of the Kansas LiDAR scanning missions have increased over time. Table 4.1 presents the reported horizontal and vertical accuracy for each year. The surveys conducted in 2009, 2010, and 2011 are suitable for the construction of 2-ft contours. These data represent an invaluable resource for hydrologic and hydraulic studies, as well as for preliminary highway planning and geometrics. The 2011 survey meets FEMA requirements for flood plain modeling and mapping.

TABLE 4.1
Horizontal and Vertical Accuracy of County-Wide LiDAR Data in Kansas

Year	Vertical RMSE (cm)	Horizontal RMSE (cm)	Cell Size (m)
2006	15	100	2
2009	18.5	60	1
2010	18.0	60	1
2011	12.5	< 60	1

Figures 4.2 and 4.3 compare the level of detail in a USGS 1 arc-second DEM and LiDAR data acquired for Atchison County, Kansas, during the 2010 campaign. Detailed LiDAR data permit accurate watershed delineation for small watersheds (see Figure 4.4) and stream channel delineation even in areas with heavy forest cover (see Figures 4.5 and 4.6).

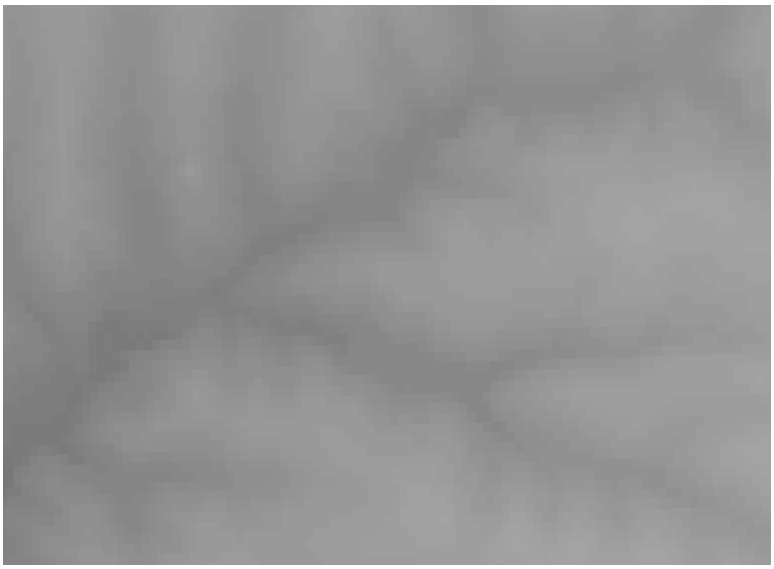

FIGURE 4.2
USGS 1 Arc-Second DEM from the National Elevation Dataset

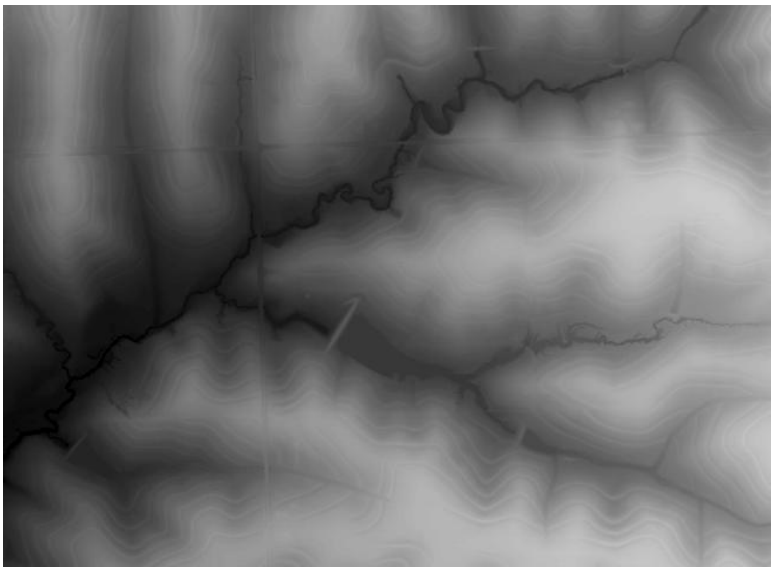

FIGURE 4.3
1-m, LiDAR-Generated DEM from Atchison County, Kansas

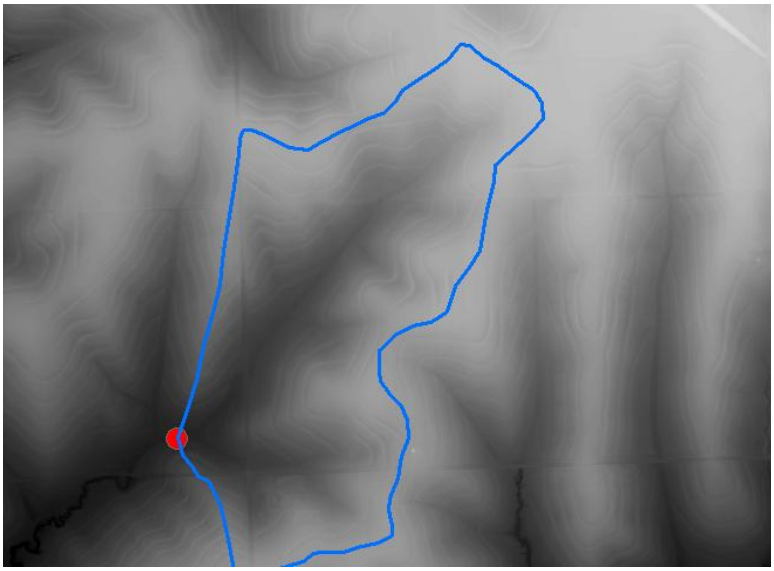

FIGURE 4.4
LiDAR-Generated DEM Used for Watershed Delineation

FIGURE 4.5
Heavily Wooded Area. Stream Channel Is Obscured.

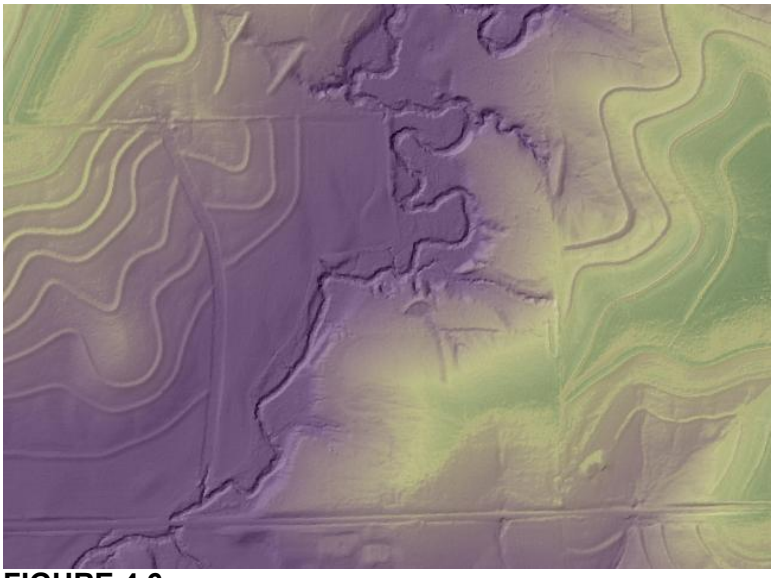

FIGURE 4.6
LiDAR Map of Stream Channel. This Is the Same Location As Shown in Figure 4.5, but LiDAR Is Able to Map Out Stream Channel with Excellent Detail

Chapter 5: Conclusions

5.1 Advantages of LiDAR Data

The most frequently-cited advantages of LiDAR data acquisition are:

1. Data density: LiDAR permits the rapid acquisition of millions of data points. Most of the error analyses cited above compare LiDAR elevations to surveyed ground elevations at the location of the surveyed point. This comparison may be erroneous. In many cases, interpolation is performed to generate a surface map between surveyed ground elevations. This interpolation introduces uncertainty that increases exponentially with distance from the surveyed datapoints.

2. Unanticipated measurements: The increased data density in LiDAR surveys permits measurements that may have been unanticipated at the time of the data acquisition. For example, a highway scan collected to determine pavement thickness may be used at a later date to analyze line-of-sight conditions for an accident.

3. Safety: LiDAR surveys can be conducted at a safe distance from moving traffic, eliminating or at least reducing exposure of survey personnel (Veneziano et al. 2004). This advantage is true for ALS, MLS, and TLS.

4. Inaccessible areas: LiDAR surveys can be conducted for areas that may be difficult to access. For example: wetlands, hazardous locations, and property where the DOT does not have landowner permission (Al-Durgham et al. 2010).

5. Heavily vegetated areas: Although LiDAR penetration to the ground is reduced in areas of dense vegetation, research has shown that ground returns are still achieved. This is particularly true for ALS surveys (Baltsavias 1999).

6. Surfaces with little texture or poor definition: LiDAR will be more accurate than photogrammetry in regions with little texture or poor definition, such as snow, ice, swamps, wetlands, and sand (Baltsavias 1999).

7. Mapping of long, narrow features (e.g., highway or rail corridors): ALS generally covers a narrower swath than photogrammetry. Photogrammetric surveys require imagery to either side of the corridor in order to interpret ground elevations. This makes LiDAR more cost effective for mapping narrow features (Baltsavias 1999).

8. Structure mapping: LiDAR will outperform photogrammetry for the mapping of three dimensional structures. For example, mapping of urban areas, bridges, or vertical objects in the right-of-way (Baltsavias 1999).

9. Very small objects: LiDAR is ideal for mapping very small objects, such as power lines (Baltsavias 1999). This technology has been embraced by the power industry, which regularly uses ALS to inventory electric transmission equipment and to conduct vegetation intrusion surveys. DOT applications may include mapping of signs, towers, trees, etc., in the right-of-way.

10. Time and cost savings: LiDAR permits rapid acquisition of data for large areas. Unlike photogrammetry, LiDAR is not limited to narrow windows for data collection. Photogrammetric surveys in vegetated areas require a leaf-off condition, daylight, and sun angle greater than 30 degrees (Veneziano et al. 2004). In many cases, these restrictions can delay the acquisition of elevation maps for months. In addition, the post-processing of LiDAR data can be conducted much faster than photogrammetric processing (Baltsavias 1999). This is due to the high degree of automation that can be employed to generate bare-earth DTMs from LiDAR point clouds.

Veneziano et al. (2002) estimated a 71% reduction in time for the generation of elevation maps using ALS compared to photogrammetric mapping (five months compared to two years for a 46-mi corridor in Iowa). Hybrid LiDAR and photogrammetry led to a thirteen month data collection project. The cost breakdown for the Iowa survey was $500,000 for photogrammetry, $150,000 for LiDAR only, and $250,000 for a hybrid LiDAR and photogrammetry survey.

Langston and Walker (2001) used helicopter-based LiDAR to collect elevation data over a 42 mi long and 1500 ft wide corridor. They estimate a cost savings of $1.5 million and a time savings of 9 months as compared to conventional methods.

Stone (1999) estimated $7 million savings in construction costs of the Hardin Canal due to LiDAR data collection.

5.2 Limitations

Laser scanning technology is not appropriate for all survey applications. The primary limitations of LiDAR surveys are:

1. Error/Uncertainty: The general consensus is that a carefully planned and executed ALS survey will generate ground elevation maps with an RMSE of 15 cm. Interestingly, this RMSE has not improved dramatically over the past 10-15 years; however, new technology and techniques promise to improve ALS accuracy to sub-decimeter levels. Recent data from Vincent and Ecker (2010) demonstrate that sub-decimeter accuracy is possible with existing technology. This level of accuracy requires careful planning, low flight elevations, and good conditions.

2. Need for excellent ground-truthing: LiDAR data acquisition should be carried out in conjunction with ground-based methods (total station or RTK-GPS) in order to supplement ground measurements. LiDAR cannot be relied upon to provide the sole source of elevation data.

3. Remote sensing: Laser scanning is by definition a remotely-sensed product. In some cases, physical measurement is necessary and cannot be replaced.

4. Post-processing requirements: Although LiDAR post processing is less intensive than photogrammetry, post processing makes up a significant portion of the expense of LiDAR surveying (often 8-10 times the duration of the data acquisition phase).

5. Data storage: LiDAR surveys rapidly produce millions or even billions of data points. As a result, data storage for active projects must be increased. Data storage and archive procedures must be developed to ensure that data are stored in a format that will be accessible for decades to come. It is recommended that both raw and final point clouds be stored in a simple text format for this purpose. Raw point clouds should be archived to allow analysis in the future using new techniques or for uses that were unanticipated at the time of the original survey.

5.3 Conclusions

LiDAR data acquisition and analysis have the potential to revolutionize highway design, construction, and maintenance. ALS surveys may be suitable to replace or supplement traditional survey and photogrammetric mapping for a variety of applications, including highway planning and hydrologic / hydraulic studies. ALS has demonstrated potential for the development of

highway inventories, sight distance studies, intersection line-of-sight studies, and the mapping of road breaklines (edge-of-curb for planimetric mapping). Currently, the accuracy of ALS is at or near 15 cm vertical RMSE, suitable for generating 2-ft contours. Recent studies have produced lower vertical RMSE, even below 10 cm. ALS is currently capable of routinely producing DEMs suitable for floodplain mapping according to FEMA standards.

MLS technology could be integrated with KDOT's current highway video collection system for documentation of road conditions. MLS has the potential to generate extremely high-resolution maps of the highway surface and adjacent corridor. These MLS data can be used for as-built documentation, development of sign inventories, or to collect preliminary elevations for design work.

TLS has tremendous potential for DOT applications, particularly when integrated with traditional survey techniques. TLS has been demonstrated to be useful for bridge clearance measurement and damage detection. An archive of bridge scans would be useful for rapid damage analysis. TLS can be used to supplement traditional survey to collect detailed elevation maps of areas that are difficult or unsafe to survey. For example, some surveying companies use LiDAR to survey intersections. MLS should be considered carefully as an alternative to TLS, as the accuracy of the two methods are similar for areas where multiple TLS scanner positions are required.

This report presents an overview of LiDAR technology, applications, and error characteristics. Over fifty research papers and reports were reviewed; these results were integrated with KU's experience with a TLS.

References

Adams, J. C., and Chandler, J. H. 2002. "Evaluation of LiDAR and Medium Scale Photogrammetry for Detecting Soft-Cliff Coastal Change." *Photogramm Rec* 17 (99): 405–418.

Al-Durgham, M., Fotopoulos, G., and Glennie, C. 2010. "On the Accuracy of LiDAR Derived Digital Surface Models." *Gravity, Geoid and Earth Observation* 689–695.

Bailly, J. S., Le Coarer, Y., Languille, P., Stigermark, C. J., and Allouis, T. 2010. "Geostatistical Estimations of Bathymetric LiDAR Errors on Rivers." *Earth Surface Processes and Landforms* 35 (10): 1199–1210.

Baltsavias, E. P. 1999. "A Comparison Between Photogrammetry and Laser Scanning." *ISPRS Journal of Photogrammetry and Remote Sensing* 54 (2–3): 83–94.

Berg, R., and Ferguson, J. 2000. "A Practical Evaluation of Airborne Laser Mapping for Highway Engineering Surveys." *Proc., ION-GPS 2000*, 1854–1864.

Bethel, J. S., Johnson, S. D., Shan, J., van Gelder, B. H. W., McCullouch, B., Cetin, A. F., Han, S., Hawarey, M., Lee, C., and Sampath, A. 2005. "Modern Technologies for Design Data Collection." Purdue University, 129.

Bowen, Z. H., and Waltermire, R. G. 2002. "Evaluation of Light Detection and Ranging (LiDAR) for Measuring River Corridor Topography." *J Am Water Resour As* 38 (1): 33–41.

Brinkman, R., and O'Neill, C. 2000. "LiDAR and Photogrammetric Mapping." *Military Engineer* 56–57.

Brook, A., Ben-Dor, E., and Richter, R. 2010. "Fusion of Hyperspectral Images and LiDAR Data for Civil Engineering Structure Monitoring." IEEE 1–5.

Carter, W., Shrestha, R., Tuell, G., Bloomquist, D., and Sartori, M. 2001. "Airborne Laser Swath Mapping Shines New Light on Earth's Topography." *EOS, Transactions American Geophysical Union*, 82 (46): 549–555.

Cobby, D. M., Mason, D. C., and Davenport, I. J. 2001. "Image Processing of Airborne Scanning Laser Altimetry Data for Improved River Flood Modelling." *ISPRS Journal of Photogrammetry and Remote Sensing* 56 (2): 121–138.

Cowen, D. J., Jensen, J. R., Hendrix, C., Hodgson, M., Schill, S. R., and Macchiaverna, F. 2000. "A GIS-Assisted Rail Construction Econometric Model that Incorporates LiDAR Data." *Photogrammetric Engineering and Remote Sensing* 66 (11): 1323–1328.

Evans, J. S., and Hudak, A. T. 2007. "A Multiscale Curvature Algorithm for Classifying Discrete Return LiDAR in Forested Environments." *IEEE Transactions on Geoscience and Remote Sensing* 45 (4): 1029–1038.

Falkowski, M. J., Evans, J. S., Martinuzzi, S., Gessler, P. E., and Hudak, A. T. 2009. "Characterizing Forest Succession with LiDAR Data: An Evaluation for the Inland Northwest, USA." *Remote Sens Environ* 113 (5): 946–956.

FEMA. 2012. "LIDAR Specifications for Flood Hazard Mapping." <http://www.fema.gov/plan/prevent/fhm/lidar_4b.shtm>.

Flood, M. 2004. "ASPRS Guidelines: Vertical Accuracy Reporting for LiDAR Data." *American Society for Photogrammetry and Remote Sensing* 20.

Glennie, C. 2007. "Rigorous 3D Error Analysis of Kinematic Scanning LiDAR Systems." *Journal of Applied Geodesy* 1 (3): 147.

Hans, Z., Tenges, R., Hallmark, S., Souleyrette, R., and Pattnaik, S. 2003. "Use of LiDAR-Based Elevation Data for Highway Drainage Analysis: A Qualitative Assessment." Midwest Transportation Consortium, Center for Transportation Research and Education, Iowa State University, Ames, Iowa, 50.

Herrs, A. J. 2010. "Quantifying Surface Subsidence along US Highway 50, Reno County, KS Using Terrestrial LiDAR." M.S., University of Kansas.

Hilldale, R. C., and Raff, D. 2008. "Assessing the Ability of Airborne LiDAR to Map River Bathymetry." *Earth Surface Processes and Landforms* 33 (5): 773–783.

Hinks, T., Carr, H., and Laefer, D. F. 2009. "Flight Optimization Algorithms for Aerial LiDAR Capture for Urban Infrastructure Model Generation." *Journal of Computing in Civil Engineering* 23 (6): 330–339.

Hodgson, M. E., and Bresnahan, P. 2004. "Accuracy of Airborne LiDAR-Derived Elevation: Empirical Assessment and Error Budget." *Photogrammetric Engineering and Remote Sensing* 70 (3): 331–339.

Hodgson, M. E., Jensen, J. R., Schmidt, L., Schill, S., and Davis, B. 2003. "An Evaluation of LiDAR- and IFSAR-Derived Digital Elevation Models in Leaf-on Conditions with USGS Level 1 and Level 2 DEMs." *Remote Sens Environ* 84 (2): 295–308.

Huising, E. J., and Pereira, L. M. G. 1998. "Errors and Accuracy Estimates of Laser Data Acquired by Various Laser Scanning Systems for Topographic Applications." *ISPRS Journal of Photogrammetry and Remote Sensing* 53 (5): 245–261.

Khatri, D. K., Han, J., Parsons, R. L., Young, B., Corey, R., and Brennan, J. 2012. "Laboratory Evaluation of Deformations of Steel-Reinforced High-Density Polyethylene Pipes Under Static Loads." *Proceedings TRB 91st Annual Meeting*.

Khattak, A. J., Hallmark, S., and Souleyrette, R. 2003. "Application of Light Detection and Ranging Technology to Highway Safety." *Transportation Research Record* 1836: 7–15.

Khattak, A. J., and Shamayleh, H. 2005. “Highway Safety Assessment Through Geographic Information System-Based Data Visualization.” *Journal of Computing in Civil Engineering* 19 (4): 407–411.

Kraus, K., and Pfeifer, N. 1998. “Determination of Terrain Models in Wooded Areas with Airborne Laser Scanner Data.” *ISPRS Journal of Photogrammetry and Remote Sensing* 53 (4): 193–203.

Lato, M., Hutchinson, J., Diederichs, M., Ball, D., and Harrap, R. 2009. “Engineering Monitoring of Rockfall Hazards Along Transportation Corridors: Using Mobile Terrestrial LiDAR.” *Nat Hazard Earth Sys* 9 (3): 935–946.

Liu, W., Chen, S., and Hauser, E. 2011. “LiDAR-Based Bridge Structure Defect Detection.” *Experimental Techniques* 35 (6): 27–34.

Liu, W., Chen, S. E., and Hasuer, E. 2011. “Bridge Clearance Evaluation Based on Terrestrial LiDAR Scan.” *Journal of Performance of Constructed Facilities* 1: 135.

Liu, W., Chen, S. E., and Hauser, E. “Remote Sensing for Bridge Health Monitoring.” 74560D.

O'Hara, C. G. “Remote Sensing and Geospatial Application for Wetland Mapping, Assessment, and Mitigation.” *Proc., ISPRS Commission I Mid-Term Symposium: Integrated Remote Sensing at the Global, Regional and Local Scale*.

Parr, A. D. 2012. *Unsteady Flow Analysis of Relief Bridges (DRAFT)*. University of Kansas, Kansas Department of Transportation, 105.

Paska, E., and Ray, J. A. 2007. “Influence of Various Parameters on the Accuracy of LiDAR Generated Products for Highway Design Applications.” *Proc., ASPRS 2007 Annual Conference* 7–11.

Pereira, L. M. G., and Janssen, L. L. F. 1999. “Suitability of Laser Data for DTM Generation: A Case Study in the Context of Road Planning and Design.” *ISPRS Journal of Photogrammetry and Remote Sensing* 54 (4): 244–253.

Pereira, L. M. G., and Wicherson, R. J. 1999. “Suitability of Laser Data for Deriving Geographical Information - A Case Study in the Context of Management of Fluvial Zones.” *ISPRS Journal of Photogrammetry and Remote Sensing* 54 (2–3): 105–114.

Pu, S., Rutzinger, M., Vosselman, G., and Elberink, S. O. 2011. “Recognizing Basic Structures from Mobile Laser Scanning Data for Road Inventory Studies.” *ISPRS Journal of Photogrammetry and Remote Sensing* 66 (6): S28–S39.

Resop, J. P., and Hession, W. C. 2010. “Terrestrial Laser Scanning for Monitoring Streambank Retreat: Comparison with Traditional Surveying Techniques.” *J Hydraul Eng-Asce* 136 (10): 794–798.

Shatnawi, F. M., and Goodall, J. L. 2010. “Comparison of Flood Top Width Predictions Using Surveyed and LiDAR-Derived Channel Geometries.” *J Hydrol Eng* 15 (2): 97–106.

Shrestha, R., Carter, W., Thompson, P., Dean, R., and Harrell, H. 1997. “Coastal and Highway Mapping by Airborne Laser Swath Mapping Technology.” *Proc., Third International Airborne Remote Sensing Conference and Exhibition - Development, Integration, Applications & Operations* I-632–I-639.

Skaloud, J., Schaer, P., Stebler, Y., and Tome, P. 2010. “Real-Time Registration of Airborne Laser Data with Sub-Decimeter Accuracy.” *ISPRS Journal of Photogrammetry and Remote Sensing* 65 (2): 208–217.

Straatsma, M. W., and Baptist, M. 2008. “Floodplain Roughness Parameterization Using Airborne Laser Scanning and Spectral Remote Sensing.” *Remote Sens Environ* 112 (3): 1062–1080.

Tao, C. V., and Hu, Y. 2002. “Assessment of Airborne LiDAR and Imaging Technology for Pipeline Mapping and Safety Applications.” *Proc., Pecora 15/Land Satellite Information IV/ISPRS Commission I/FIEOS 2002: Integrating Remote Sensing at the Global, Regional and Local Scale*, Citeseer.

Toth, C. K., and Grejner-Brzezinska, D. 2006. “Extracting Dynamic Spatial Data from Airborne Imaging Sensors to Support Traffic Flow Estimation.” *ISPRS Journal of Photogrammetry and Remote Sensing* 61 (3–4), 137–148.

Uddin, W. 2002. “Evaluation of Airborne LiDAR Digital Terrain Mapping for Highway Corridor Planning and Design.” *Proc. Pecora* 15: 10–15.

Veneziano, D., Hallmark, S., and Souleyrette, R. 2002. “Comparison of LiDAR and Conventional Mapping Methods for Highway Corridor Studies.” Center for Transportation Research and Education Iowa State University, Ames, Iowa, 58.

Veneziano, D., Hallmark, S., and Souleyrette, R. 2004. “Accuracy of Light Detection and Ranging Derived Terrain Data for Highway Location.” *Comput-Aided Civ Inf* 19 (2): 130–143.

Veneziano, D., Souleyrette, R., and Hallmark, S. 2002. “Evaluation of LiDAR for Highway Planning, Location and Design.” *Proc. Pecora* 15.

Vincent, R., and Ecker, M. 2010. “Light Detection and Ranging (LiDAR) Technology Evaluation.” Sanborn Map Company, HDR Engineering, and Missouri Department of Transportation 104.

Walters, R., Jaselskis, E., Zhang, J. Z., Mueller, K., and Kaewmoracharoen, M. 2008. “Using Scanning Lasers to Determine the Thickness of Concrete Pavement.” *J Constr Eng M ASCE* 134 (8): 583–591.

Watson, C., Chen, S. E., Bian, H., and Hauser, E. 2011. "LiDAR Scan for Blasting Impact Evaluation on a Culvert Structure." *Journal of Performance of Constructed Facilities* 1: 227.

Wolf, D., Eadie, R., and Kyzer, J. 2000. "Digital Photography/LiDAR of Archeo/Paleo Sites on the Comanche National Grassland." *Proc USFS Remote Sensing Conference*.

Young, C. B. 2011. "Establishing Baseline Topography for the Long-Term Evaluation of Stream Stabilization Efforts on the Neosho River." University of Kansas, Unpublished Report to the Kansas Water Office.

Zhou, L., and Vosselman, G. 2012. "Mapping Curbstones in Airborne and Mobile Laser Scanning Data." *International Journal of Applied Earth Observation and Geoinformation* 18: 293–304.

K-TRAN

KANSAS TRANSPORTATION RESEARCH AND NEW-DEVELOPMENT PROGRAM

AD ASTRA PER ASPERA

Kansas

Department of Transportation